PLOS One

RESEARCH ARTICLE

HPLC-MS profiling and protective potential of the defatted aqueous methanol extract of two *Syzygium* species against cadmium chloride-induced nephrotoxicity in rats

Fatma A. Moharram[1☯], Sahar S. Salem[2☯], Samah Shabana[2], Elsayed K. El-Sayed[3], Shimaa K. Mohamed[3], Mohamed A. Khattab[4], Kuei-Hung Lai[5,6,7*], Asmaa A. Ahmed[3], Heba E. Elsayed[1]

1 Department of Pharmacognosy, Faculty of Pharmacy, Helwan University, Cairo, Egypt, **2** Department of Pharmacognosy, Faculty of Pharmaceutical Science and Drug Manufacturing, Misr University for Science and Technology, Giza, Egypt, **3** Department of Pharmacology and Toxicology, Faculty of Pharmacy, Helwan University, Cairo, Egypt, **4** Department of Cytology and Histology, Faculty of Veterinary Medicine, Cairo University, Giza, Egypt, **5** Graduate Institute of Pharmacognosy, College of Pharmacy, Taipei Medical University, Taipei, Taiwan, **6** PhD Program in Clinical Drug Development of Herbal Medicine, College of Pharmacy, Taipei Medical University, Taipei, Taiwan, **7** Traditional Herbal Medicine Research Center, Taipei Medical University Hospital, Taipei, Taiwan

☯ These authors contributed equally to this work.
* kueihunglai@tmu.edu.tw

OPEN ACCESS

Citation: Moharram FA, Salem SS, Shabana S, El-Sayed EK, Mohamed SK, Khattab MA, et al. (2025) HPLC-MS profiling and protective potential of the defatted aqueous methanol extract of two *Syzygium* species against cadmium chloride-induced nephrotoxicity in rats. PLoS One 20(8): e0329586. https://doi.org/10.1371/journal.pone.0329586

Editor: Saikat Dewanjee, Jadavpur University, INDIA

Received: April 14, 2025

Accepted: July 16, 2025

Published: August 14, 2025

Data availability statement: All available data are presented in the paper.

Funding: The grants from the National Science and Technology Council of Taiwan (MOST 111-2321-B-255-001 and MOST

Abstract

Cadmium (Cd), a highly toxic heavy metal, is used in food and agricultural products while displaying nephrotoxicity to animals and humans. The genus *Syzygium* (Myrtle family) is rich in precious phenolic metabolites with various therapeutic values. This study investigated the phenolic content and the therapeutic potential of the defatted 80% aqueous methanol extract (DE) of *S. malaccense* and *S. samarangense* leaves against Cd-induced kidney injury in rats for the first time. High-performance liquid chromatography-Mass spectrometry (HPLC-MS), in addition to Folin-Ciocalteu and aluminium chloride colourimetric methods, depicted the phenolic metabolites, total phenolic content, and total flavonoid content, respectively. The nephroprotective effect was investigated using fifty-six female *Sprague Dawley* rats divided into eight groups: control group, $CdCl_2$-treated group (3 mg/kg/i.p/7 days), and three groups of each species treated with the DE (250, 500, and 1000 mg/kg/o.p., respectively). The phytochemical analysis revealed the richness of *S. samarangense* DE by phenolic and flavonoid content over *S. malaccense*. The HPLC-MS showed the tentative identification of sixty-two compounds, in positive and negative ionization modes, belonging to phenolic acids **(1−6**), flavonoids **(7−52),** and miscellaneous compounds **(53−62)**. Both extracts were considered safe up to 5 g/kg. At the maximum tested dose (100 mg/Kg), the DEs significantly ($p < 0.001$) boosted the levels of antioxidant markers by 3.3–6 fold, lessened the inflammatory indicators by 66.8%−75.1%, and reduced the apoptotic parameters by 45.4–73.3%, compared to the $CdCl_2$-treated

111-2320-B-038-040-MY3) supported this work.

Competing interests: The authors have declared that no competing interests exist.

group. Additionally, the DEs maintained the mitochondrial function and inhibited autophagy *via* decreasing adenosine monophosphate-activated protein kinase by 49.2%−50.6%, and baclin-1 by 49.5%−56.1%. Additionally, the DEs increased the mammalian target of rapamycin (mTOR) by 4.7–4.9 fold. Additionally, the DE ameliorated CdCl2-induced elevations in serum ALT and AST, indicating a protective effect against systemic toxicity. Ultimately, the DE of *S. malaccense* and *S. samarangense* protect against Cd-induced nephrotoxicity that may be correlated to their abundant phenolic content. However, selecting suitable formulations and implementing clinical studies are among the future directions.

Introduction

Cadmium (Cd) is a hazardous heavy metal renowned for its toxic potential to the kidneys [1]. Humans may be at risk from two types of Cd exposure. On top is the occupational Cd exposure through engaging with industrial activities [2] in addition to non-occupational exposure *via* contaminated food and water [3]. After Cd-exposure, multifactorial mechanisms are implicated in the pathogenesis of Cd-toxicity, such as oxidative stress, mitochondrial dysfunction, apoptosis, and inflammation [4–6]. Moreover, autophagy pathways are considered sensitive biomarkers for kidney damage upon Cd intoxication [7,8]. Currently, there is no standard therapy for Cd-induced nephrotoxicity, which underscores the urgent demand for the scientific community to discover a promising treatment, particularly given the growing global interest in the therapeutic values of antioxidants [9].

Phenolic compounds are a miscellaneous group of plant-derived metabolites that include different subclasses. They possess a unique chemical scaffold with potent antioxidant and anti-inflammatory activities [10–12]. Since oxidative stress and inflammation play essential roles in the prognosis of kidney diseases, phenolic metabolites offer potential as natural mediators that can modify these pathological processes [13–19]. Several plants are abundant in phenolics, including but not limited to *Syzygium* species (Myrtle family) [20,21]. Among the limitley explored species are *Syzygium malaccense* (L.) Merr. & L. M. Perry and *Syzygium samarangense* (Blume) Merr. & L. M. Perry. They are distributed in tropical and subtropical regions of Africa and Asia, and are renowned for their edible fruits [21–24]. In traditional medicine, *S. malaccense* was used as an anti-inflammatory, while the leaves and fruits were pharmacologically proven to possess anti-microbial and antioxidant activities, at least in part, due to their phenolic composition [25–31]. Extracts of *S. samarangense* displayed anti-inflammatory, analgesic, hepatoprotective, and diuretic effects [21,32]. These pharmacological activities are attributed to different classes of phenolic metabolites [21,33–35]. Although some biological activities were reported for *S. malaccense* and *S. samarangense*, their potential protective effect against Cd-induced nephrotoxicity has not been reported. Hence, encouraging our research team in the current study to investigate their nephroprotective potential.

Plant extracts represent a complex mixture of hundreds of diverse metabolites [36], making their analysis a challenging task. Although different chromatographic and spectroscopic approaches are available, high-performance liquid chromatography-mass spectrometry (HPLC-MS) permits comprehensive extract analysis on its own [37]. As a state-of-the-art analytical coupling approach, it merges the efficient separation aptitudes of HPLC with the supreme sensitivity and specificity of MS [37]. Hence, it provides valuable and prompt structural information on the metabolites detected without the need for isolation. Additionally, it is noticeable by its applicability to varied analyte types (ranging from small molecules to large polymers), providing higher resolution, greater sensitivity, and precision [36,37].

In the current study, we aimed to profile the phenolic content and composition of the defatted aqueous methanol extract of *S. malaccense* and *S. samarangense* using HPLC-MS. In addition, we evaluated their nephroprotective activity in a Cd-induced nephrotoxicity *in vivo* model.

Materials and methods

Plant material

Syzygium malaccense (L.) Merr. & L. M. Perry and *Syzygium samarangense* (Blume) Merr. & L. M. Perry leaves were supplied (June to August 2021) from Mazhar Botanical Garden, Cairo, Egypt. The plants were collected after the garden authorities' permission, following the local garden`s guidelines for collection under the supervision of Dr. Trease Labib, a senior botanist at Mazhar Botanical Garden, who confirmed the species' identity and the species' names following the International Plant Name Index (IPNI). Samples from each species were kept in the Pharmacognosy Department, Faculty of Pharmacy, Helwan University under the numbers 01Sma, 2021, and 01Ssa, 2021. The plant material under study is endotoxin-free, and the study protocol was approved by the Ethics Committee of the Faculty of Pharmacy, Helwan University (Approval No: 11A2023).

Chemicals and reagents

Methanol, *n*-hexane, normal saline, buffered formalin, and phosphate buffer were supplied from El Nasr Pharmaceutical Chemicals Co. (Gesr El Suez, Cairo, Egypt). Folin-Ciocalteu reagent, gallic acid, catechin, $AlCl_3$, anhydrous cadmium chloride ($CdCl_2$), ethanol, sodium thiopental, and hematoxylin-eosin staining solution were obtained from Sigma-Aldrich Inc. (St. Louis, MO, United States).

Preparation of the defatted extract (DE)

S. malaccense (275 g) and *S. samarangense* (230 g) leaves were individually extracted with 80% aqueous methanol under reflux (3 x 4 L). The filtered, pooled extracts were evaporated under reduced pressure (60°C) to yield 35.0 g and 22.0 g of *S. malaccense* and *S. samarangense* dry extracts, respectively. The extracts were defatted by *n*-hexane under reflux (3 x 1 L) followed by solvent evaporation under *vacuum* using a rotary evaporator, followed by lyophilization to yield 10.0 g and 7.0 g (*n*-hexane) and 20.0 g and 10.0 g (defatted extract, DE) for *S. malaccense* and *S. samarangense,* respectively. The dried DE from each species was subjected to quantitative and qualitative phenolic profiling, and we investigated its protective potential in the Cd-induced nephrotoxicity *in vivo* model. The remainder of the extract was kept in a well-sealed container at −80°C.

Estimation of total phenolic content (TPC)

It was estimated following the Folin-Ciocalteu colorimetric method [38]. The absorbance was determined at 725 nm on a UV-visible spectrophotometer (Jasco V-730, Jasco Corporation, Japan). The results were calculated from the calibration curve of the standard (gallic acid 50–300 µg/mL) using the following equation:

$$y = 0.0237x + 0.0455\ (R^2 = 0.9976)$$

The results were stated as gallic acid (mg) equivalent (mg GAE/mg) of dry weight.

Estimation of total flavonoid content (TFC)

It was measured colorimetrically using the $AlCl_3$ [38]. The absorbance was measured at 510 nm on a UV-visible spectrophotometer (Jasco V-730, Jasco Corporation, Japan). The results were deduced from the equation of the calibration curve constructed from the standard (catechin, 50–300 µg/mL) as follows:

$$y = 0.0088x + 0.0430\ (R^2 = 0.9994)$$

Results were expressed as milligrams of catechin equivalent (mg CE/mg of dry weight).

Determination of phenolic profile using HPLC-MS

The HPLC-MS analysis was performed on the XEVO® triple quadrupole (TQD) mass system (Waters™ Corporation, Milford, MA, United States) operated in negative and positive ionization modes. Chromatographic separation was carried out on the ACQUITY UPLCBEH C18 column (1.7 µm x 2.1 mm x 50 mm, 28.4 °C) using 0.1% formic acid in H_2O as solvent A and MeOH as solvent B. Isocratic gradient elution was implemented using a flow rate of 0.2 mL/min for 32 min as follows: 10% B for 5 min, 30% B for 10 min, 70% B for 7 min, then 90% B for 10 min. The MS acquisition range was *m*/*z* 50–1000.

In vivo nephrotoxic activity induced by cadmium chloride ($CdCl_2$)

Experimental animals. Adult female Sprague-Dawley rats (9–10 weeks old, 180–200 g) were purchased from 223 VACSERA (Helwan, Cairo, Egypt). Rats were housed (3–4 rats/cage) at a controlled 224 temperature of 22°C ± 3°C with a 12-hour light/dark cycle. Standard rodent chow and water were provided ad libitum. All procedures were conducted following the ethical standards approved by the Ethics Committee of the Faculty of Pharmacy, Helwan University (Approval No: 11A2023). The study was conducted in compliance with the ARRIVE guidelines 2.0, the EU Directive 2010/63/EU for the protection of animals used for scientific purposes, and the NIH Guide for the Care and Use of Laboratory Animals (8th edition). The experimental design included the possibility of mortality due to the nature of the pharmacological intervention. Therefore, animals were monitored at least twice daily for clinical signs of pain, distress, or illness, including reduced mobility, abnormal posture, respiratory distress, piloerection, and failure to groom. If any animal exhibited signs of severe distress or met predetermined humane endpoints (e.g., > 20% weight loss, loss of appetite > 48 hours, or unresponsiveness), it was euthanized immediately via an overdose of sodium thiopental administered intraperitoneally (≥150 mg/kg). No animals died unexpectedly, and euthanasia was performed according to ethical guidelines to minimize suffering. All efforts were made to refine procedures and reduce the number of animals used. The Humane endpoints checklist is supplied as supporting material S1.

Acute toxicity study. We used adult female rats, strain *Sprague Dawley* (180–200 g, n = 6), to establish the acute study. In a dose-dependent approach, the rats were administered *S. malaccense* DE and *S. samarangense* DE at 50 mg/kg, 200 mg/kg, 500 mg/kg, 1g/kg, 2.5 g/kg, and 5 g/kg. The rats were well observed for 24 h for any symptoms of toxicity, side effects, behavioral changes, movement patterns, diarrhea, and death.

Experimental design. Fifty-six rats were randomly divided into eight groups (n = 7). The control group received 0.9% saline solution as a vehicle for seven days. In the $CdCl_2$ group (group 2), rats were injected with $CdCl_2$ (3 mg/kg/intraperitoneal) for 7 days [39]. Animal groups 3–5 were treated for seven days with the DE of *S. malaccense* at 250, 500, and 1000 mg/kg orally, about one hour before the administration of $CdCl_2$. On the other hand, groups 6–8 were treated for seven days with the DE of *S. samarangense* at 250, 500, and 1000 mg/kg doses, respectively, about one hour

before the administration of $CdCl_2$. On the 8th day, rats were intraperitoneally injected with sodium thiopental (40 mg/kg) [40] to induce anesthesia. Blood samples were collected from the retro-orbital plexus using non-heparinized tubes. Rats were euthanized by cervical dislocation, and the kidneys were isolated, washed with cold saline, and weighed. The right kidneys were homogenized in an ice-cold phosphate buffer (10 mM, pH 7.4) to prepare tissue homogenates of 10% w/v for biochemical parameters. The left kidneys were preserved in formal saline (10%) for histopathological analysis.

Measurements of biochemical markers

Serum urea and creatinine. Urea and creatinine levels were determined using colorimetric kits (Catalog #K375-100 and K625-100, respectively) purchased from BioVision (Milpitas, United States). The colour intensity was measured on a Jenway™ 7315 spectrophotometer (Fisher Scientific, Leicestershire, UK).

Oxidative stress parameters. The levels of GSH and SOD in the kidney tissue homogenates were quantified using the colorimetric kit (Catalog #K464-100 and K335-100 respectively) obtained from BioVision (Milpitas, United States). The colour intensity was measured on a Jenway™ 7315 spectrophotometer (Fisher Scientific, Leicestershire, UK).

Inflammatory parameters. Using specific ELISA kits, the levels of TNF-*α* (Catalog # 438204, BioLegend, San Diego, United States), IL-1*β* (Catalog # E0119Ra, Bioassay Technology Laboratory, Shanghai, China), and NF-κB p65 (Catalog # ABIN1380657, Antibodies-online, Canada) were quantified in kidney tissue homogenates using NS 100 microplate reader (Heruvan Lab Systems, Selangor, Malaysia).

Apoptotic parameter. The level of the apoptotic marker, caspase-3, was determined in the kidney tissue homogenates using an ELISA kit (Catalog # E4592-100, BioVision, Milpitas, United States) and NS 100 microplate reader (Heruvan Lab Systems, Selangor, Malaysia).

Mitochondrial dysfunction parameter. The ATP level in kidney tissue homogenates was estimated using a colorimetric Kit (Catalog # ab83355, Abcam, Cambridge, United Kingdom). The colour intensity was measured on a Jenway™ 7315 spectrophotometer (Fisher Scientific, Leicestershire, UK).

Autophagic parameters. For the determination of autophagic parameters, ELISA Kits for the phosphorylated mammalian target of rapamycin (p-mTOR) (Catalog # ab279869, Abcam, Cambridge, United Kingdom), Beclin-1 (Catalog# ER0416, FineTest, Wuhan, China), and phosphorylated adenosine monophosphate-activated protein kinase (p-AMPK) (Catalog # ER0730, FineTest, Wuhan, China) were used according to the manufacturer's procedures. In brief, samples were added to their corresponding microtiter plate wells coated with the targeted monoclonal antibodies. Accordingly, any rat p-mTOR, beclin-1, or p-AMPK in the samples would bind to their corresponding immobilized antibodies. The wells were washed, and biotin-conjugated anti-rat p-mTOR, beclin-1, or p-AMPK antibodies (1:100) were added to their corresponding plates. The plates were washed, and avidin-horseradish peroxidase (avidin-HRP) was added. Then, the wells were washed, and tetramethylbenzidine (TMB) substrate solution was added to produce a blue color directly proportional to the amount of the detected proteins in the sample. The reaction was terminated by adding the stop solution, which changed the color from blue to yellow, and the intensity of the color was measured at 450 nm using an NS 100 microplate reader (Heruvan Lab Systems, Selangor, Malaysia).

Assessment of liver enzymes. To evaluate the systemic toxicity of cadmium, the serum levels of alanine aminotransferase (ALT) and aspartate aminotransferase (AST) were measured using Biomatik ELISA kits (Cat no: EKU02211, EKE62019, Kitchener, Ontario, N2C 1N6, Canada, respectively). The procedures were carried out according to the manufacturer's instructions

Histopathological analyses. Kidney tissue samples from the investigated groups were fixed in 10% neutral buffered formalin for three days. The samples underwent a series of ethanol dehydration steps, followed by xylene clearing and embedding in Paraplast embedding media. Kidney tissue sections (4 μm) were cut using a rotary microtome and then fixed on glass slides for further examination. Finally, using hematoxylin and eosin, tissue slices were stained and inspected under a light microscope [41].

Statistical analysis

All experiments were implemented in triplicate, and values were represented as mean ± SEM. Results were analyzed using ANOVA followed by Tukey's test, while the student's t-test was implemented to analyze the TPC and TFC data. The Prism software, version 8, was used for the statistical analysis (GraphPad Software Inc., San Diego, United States). *P*-value, which is less than 0.001, is statistically significant and denoted with an asterisk or a letter, as indicated.

Results

Extraction, quantification, and identification of phenolic metabolites

Quantification of phenolic and flavonoid contents from two *Syzygium* species. As stated earlier, the total phenolic and flavonoid contents in the DE of the two investigated species were measured using colourimetric assays. The results (Table 1) have shown that *S. samarangense* possesses a TPC that is 1.5-fold higher than *S. malaccense,* and the difference is statistically significant. Interestingly, this is the first study reporting the TPC for *S. samarangense.* However, it has been previously reported from *S. malaccense* by several researchers, notably ranging from 62.31 ± 8.32 to 88.73 ± 7.71 mg GAE/g [25,30]. On the other hand, *S. samarangense* showed significantly higher total flavonoid content than *S. malaccense* by 1.2-fold. This is the first report on the TFC of *S. samarangense,* although it has been quantitatively documented before (8.10 ± 46.75 CE/g) by Batista et al. [25]. The possible deviation in our data from those reported in the literature could be attributed to the geographical collection site's impact and the variations in the extraction conditions (solvent, time, and temperature) [42].

HPLC-MS analysis for defatted extract (DE) of *S. malaccense* and *S. samarangense* leaves. The HPLC-MS for the DE of the two *species* revealed the presence of sixty-two secondary metabolites belonging to various classes, which were tentatively identified in positive and negative modes (Table 2). Thirty-nine were detected in *S. malaccense*, while forty-six were in *S. samarangense*. The HPLC-MS chromatograms of the two species are displayed in Figs 1 and 2.

Phenolic acids are widely distributed in all native Australian flora, including *Syzygium* species [43]. Based on their chemical scaffold, they are sub-classified into hydroxybenzoic and hydroxycinnamic acid derivatives [44]. In the current study, we identified three hydroxybenzoic acid derivatives in the negative mode of *S. malaccense* (**1**, **2**, **6**) and five in *S. samarangense* (**1–3**, **5**, **6**). Additionally, one hydroxycinnamic acid derivative (**4**) was detected in the positive mode of *S. malaccense*. Compounds **1**, **2**, **3**, and **5**, were identified as gallic acid, methyl gallate, ellagic acid glucoside, and ellagic acid with m/z $[M-H]^-$ 169.0373, 183.0698, 463.1513, and 301.0638, respectively. Compounds **4** and **6** were identified as hydroxycaffeic acid and gallic acid glucoside with m/z $[M+H]^+$ 197.1579 and 333.1248, respectively. Compounds **1, 2, 5,** and **6** were identified before from *S. samarangense* [32,45], while compound **1** was previously reported from *S. malaccense* [30,46]. The remaining compounds were identified for the first time.

Flavonoids are the most abundant bioactive metabolites widely distributed in medicinal plants. They are crucial metabolites with favorable therapeutic effects on multiple diseases [47]. Chemically, flavonoids comprise 15 carbon atoms in their basic frame, which are allocated as two six-membered rings and one three-carbon unit coupled to them as C6-C3-C6. Based on structural differences, they are classified into seven subclasses: flavonols, flavones, isoflavones,

Table 1. Estimated total phenolic content (TPC), and total flavonoid content (TFC) in the defatted extract (DE) of *S. malaccense* and *S. samarangense* leaves.

Species	TPC (mg GAE/g)	TFC (mg CE/g)
S. malaccense	84.24 ± 0.94	6.41 ± 0.36
S. samarangense	123.70 ± 1.41*	7.83 ± 0.25*

Data represented as mean ± SEM of n = 3. *: significant from *S. malaccense* ($p < 0.001$).

https://doi.org/10.1371/journal.pone.0329586.t001

Table 2. HPLC-MS tentative identification of phenolic metabolites from the defatted extract (DE) of *S. malaccense* (SM) and *S. samarangense* (SS) leaves.

No.	Identified phenolics	Molecular formula	Retention time (min)	Mode of ionization	Molecular weight	Observed (*m*/*z*)	*SM*	*SS*	Reference
	Phenolic acids								
1	Gallic acid	$C_7H_6O_5$	1.06	$[M-H]^-$	170.12	169.0373	+	+	[32]
2	Methyl gallate	$C_8H_8O_5$	2.41	$[M-H]^-$	184.15	183.0698	+	+	[55]
3	Ellagic acid glucoside	$C_{20}H_{16}O_{13}$	5.96	$[M-H]^-$	464.333	463.1513	–	+	[49]
4	Hydroxycaffeic acid	$C_9H_8O_5$	6.19	$[M+H]^+$	169.157	197.1579	+	–	[56]
5	Ellagic acid	$C_{14}H_6O_8$	6.21	$[M-H]^-$	302.193	301.0638	–	+	[49]
6	Gallic acid glucoside	$C_{13}H_{16}O_{10}$	6.54	$[M+H]^+$	332.26	333.1248	+	+	[49]
	Flavonoids Flavonol								
7	Myricetin	$C_{15}H_{10}O_8$	5.96	$[M-H]^-$ $[M+H]^+$	318.2370	317.1821 319.0877	+	+	[35]
8	Myricetin- *O*-rhamnoside	$C_{21}H_{20}O_{12}$	5.97	$[M-H]^-$ $[M+H]^+$	464.3790	463.2279 465.1994	+	+	[46]
9	Isoquercetin	$C_21H_{20}O_{12}$	6.13	$[M-H]^-$	464.376	463.1943	–	+	[25]
10	Quercetin	$C_{15}H_{10}O_7$	6.13	$[M-H]^-$	302.236	301.0468	+	+	[46]
11	Hyperin	$C_{21}H_{20}O_{12}$	6.21	$[M-H]^-$	464.376	463.1249	–	+	[52]
12	Isorhamnetin-*O*-rhamnoside	$C_{22}H_{22}O_{11}$	6.29	$[M+H]^+$	462.4	463.1954	+	–	[46]
13	Isorhamnetin-*O*-glucoside	$C_{22}H_{22}O_{12}$	6.52	$[M-H]^-$	478.403	477.1945	+	+	[25]
14	Mearnsetin	$C_{16}H_{12}O_8$	6.52	$[M+H]^+$	332.26	333.1245	+	+	[46]
15	Quercitrin	$C_{21}H_{20}O_{11}$	6.54	$[M-H]^-$	448.377	447.2192	+	–	[46]
16	Kaempferol –*O* glucoside	$C_{21}H_{20}O_{11}$	6.54	$[M-H]^-$	448.377	447.2192	+	–	[25]
17	Quercetin 4′-*O*-glucuronide	$C_{21}H_{18}O_{13}$	6.54	$[M-H]^-$	478.36	477.2255	+	+	[49]
18	Mearnsitrin	$C_{22}H_{22}O_{12}$	6.79	$[M-H]^-$	478.4	477.2544	+	+	[46]
19	Kaempferol	$C_{15}H_{10}O_6$	14.56	$[M+H]^+$	286.2390	287.1558	+	+	[35]
20	Quercetin 3-*O*-acetyl-galactoside)-*O*-rhamnoside	$C_{29}H_{32}O_{17}$	24.21	$[M+H]^+$	652.1622	653.4450	+	–	[57]
21	Quercetin 3'-sulfate	$C_{15}H_{10}O_{10}S$	27.80	$[M+H]^+$	382.3	383.4042	–	+	[58]
	Flavone								
22	3,4',7-Tetrahydroxyflavone	$C_{15}H_{10}O_6$	14.79	$[M-H]^-$	285.0455	285.1601	–	+	[49]
23	Diosmin	$C_{28}H_{32}O_{15}$	21.29	$[M+H]^+$	608.549	609.4222	+	–	[49]
24	Apigenin-7-O-diglucuronide	$C_{27}H_{26}O_{17}$	23.91	$[M+H]^+$	622.485	623.4117	+	–	[59]
	Flavanones								
25	Pinocembrin	$C_{15}H_{12}O_4$	11.31	$[M-H]^-$ $[M+H]^+$	256.2570	255.1476 257.1037	+	+	[35]
26	Cryptostrobin	$C_{16}H_{14}O_4$	12.46	$[M-H]^-$ $[M+H]^+$	270.284	269.1739 271.0981	+	+	[32]
27	Strobopinin	$C_{16}H_{14}O_4$	12.72	$[M-H]^-$	270.2840	269.1747	–	+	[35]
28	Naringenin	$C_{15}H_{12}O_5$	13.17	$[M+H]^+$	272.257	273.2100	+	–	[46]
29	8-Methylpinocembrin	$C_{16}H_{14}O_4$	14.09	$[M+H]^+$	270.2840	271.1037	–	+	[35]
	Flavanones								
30	7-Hydroxy-5-methoxy-6,8-dimethylflavanone	$C_{18}H_{18}O_4$	15.61	$[M-H]^-$	298.3380	297.2050	–	+	[35]
31	8-Prenylnaringenin	$C_{20}H_{20}O_5$	20.45	$[M-H]^-$	340.375	339.3448	–	+	[60]
32	6-Geranylnaringenin	$C_{25}H_{28}O_5$	28.56	$[M+H]^+$	408.4868	409.4701	–	+	[49]

(Continued)

Table 2. (Continued)

No.	Identified phenolics	Molecular formula	Retention time (min)	Mode of ionization	Molecular weight	Observed (*m*/*z*)	*SM*	*SS*	Reference
	Isoflavone								
33	Biochanin A	$C_{16}H_{12}O_5$	10.44	$[M-H]^-$ $[M+H]^+$	284.263	283.1853 285.1370	+	–	[50]
34	4'-*O*-Methylequol	$C_{16}H_{16}O_3$	11.53	$[M-H]^-$	256.30	255.1296	–	+	[49]
35	Dihydrodaidzein	$C_{15}H_{12}O_4$	11.63	$[M-H]^-$	256.25	255.1142	–	+	[50]
36	Glycitin-6''-*O*-acetate	$C_{24}H_{24}O_{11}$	11.89	$[M-H]^-$	488.4	487.4554	–	+	[50]
37	Pseudobaptigenin	$C_{15}H_{10}O_7$	13.17	$[M+H]^+$	282.25	283.1075	+	–	[61]
38	Glycitein	$C_{16}H_{12}O_5$	13.96	$[M-H]^-$	284.263	283.1666	+	–	[50]
39	Genistein 4',7-*O* diglucuronide	$C_{27}H_{26}O_{17}$	28.16	$[M-H]^-$	622.485	621.4432	–	+	[62]
	Chalcones								
40	Phloretin	$C_{15}H_{14}O_5$	0.66	$[M-H]^-$	274.269	273.0029	–	+	[46]
41	6,8-Di-C-methyl pinocembrin-5-methyl ether	$C_{18}H_{18}O_4$	11.67	$[M+H]^+$	298.3380	299.1618	+	–	[35]
42	Aurentiacin	$C_{18}H_{18}O_4$	12.06	$[M-H]^-$ $[M+H]^+$	298.3380	297.1133 299.1569	+	+	[35]
43	Cardamonin	$C_{16}H_{14}O_4$	12.92	$[M-H]^-$ $[M+H]^+$	270.28	269.1631 271.1143	+	+	[52]
44	Uvangoletin	$C_{15}H_{10}O_6$	13.40	$[M-H]^-$	272.3000	271.1406	–	+	[35]
45	2',4'-Dihydroxy-3'-methyl-6'-methoxy-chalcone	$C_{17}H_{16}O_4$	13.53	$[M-H]^-$ $[M+H]^+$	284.3065	283.1888 285.2387	+	+	[51]
46	Stercurensin	$C_{17}H_{16}O_4$	13.77	$[M-H]^-$ $[M+H]^+$	284.3110	283.1625 285.1329	+	+	[35]
47	Demethoxymatteucinol	$C_{17}H_{16}O_4$	14.14	$[M-H]^-$ $[M+H]^+$	284.3110	283.1846 285.1332	+	+	[35]
48	2'-Hydroxy-4',6'-dimethoxy chalcone	$C_{16}H_{12}O_5$	14.41	$[M-H]^-$	284.307	283.2011	–	+	[49]
49	2',4'-Dihydroxy-6'-methoxy-3'-methyl dihydrochalcone	$C_{17}H_{18}O_4$	14.65	$[M-H]^-$ $[M+H]^+$	286.3270	285.2119 287.1356	+	+	[35]
50	2′,4′-Dihydroxy-6′- methoxy3′,5′- dimethyl dihydrochalcone	$C_{18}H_{18}O_4$	15.35	$[M-H]^-$ $[M+H]^+$	298.3	297.2200 299.1672	+	+	[63]
51	4',6'-Dihydroxy-3',5'-dimethyl-2'-methoxy chalcone	$C_{18}H_{18}O_4$	15.45	$[M-H]^-$	298.3380	297.1987	–	+	[35]
52	Dimethyl cardamonin	$C_{18}H_{18}O_4$	15.81	$[M-H]^-$ $[M+H]^+$	298.331	297.2204 299.1618	+	+	[64]
	Lignin								
53	Lariciresinol-sesquilignan	$C_{30}H_{36}O_{10}$	15.82	$[M-H]^-$	556.601	555.4398	+	–	[49]
	Resorcinol derivatives								
54	5-Heptadecylresorcinol	$C_{23}H_{40}O_2$	7.46	$[M-H]^-$ $[M+H]^+$	348.56	347.2201 349.2050	+	–	[54]
55	Adipostatin E	$C_{22}H_{38}O_2$	7.67	$[M-H]^-$	334.544	333.2106	+	–	[54]
	Others								
56	Bergapten	$C_{12}H_8O_4$	0.72	$[M-H]^-$	216.189	215.1005	–	+	[65]
57	Citric acid	$C_6H_8O_5$	0.72	$[M-H]^-$	192.124	191.0651	–	+	[46]
58	Malic acid	$C_4H_6O_5$	0.75	$[M-H]^-$	134.0874	132.9923	+	+	[46]
59	Quinic acid	$C_7H_{12}O_6$	0. 80	$[M-H]^-$	192.17	191.1055	+	+	[32]
60	3,5-Dimethyl-resveratrol (Pterostilbene)	$C_{16}H_{16}O_3$	11.79	$[M-H]^-$	256.3	255.1323	–	+	[66]
61	Stigmastanol, *trans*-ferulate	$C_{39}H_{60}O_4$	21.93	$[M+H]^+$	592.4488	593.3953	+	–	[67]
62	Cyanidin-3-*O*-glucosyl-rutinoside	$C_{33}H_{41}O_2$	31.05	$[M+H]^+$	757.2184	758.7891	–	+	[68]

https://doi.org/10.1371/journal.pone.0329586.t002

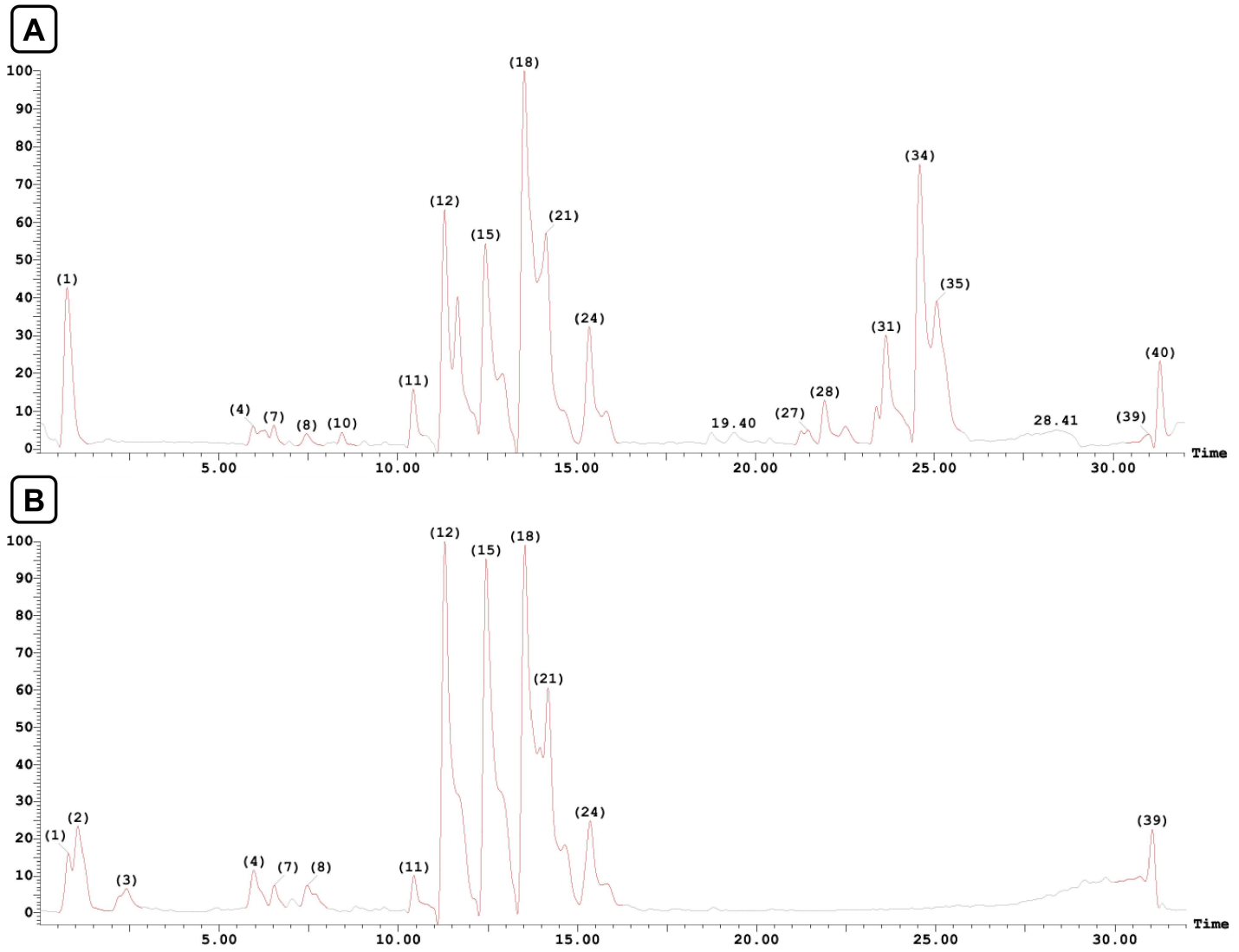

Fig 1. Total ion chromatogram (TIC) obtained from HPLC-MS of the defatted aqueous methanol extract of *S. malaccense* leaves in (A) positive and (B) negative ionization modes.

https://doi.org/10.1371/journal.pone.0329586.g001

anthocyanidins, flavanones, flavanols, and chalcones [48]. In the current study, we annotated **46** flavonoids, including **15** flavonols, **7** flavanones, **3** flavones, 7 isoflavonoids, and 14 chalcones (Table 2).

Another notable subclass of flavonoids is the flavonols. Herein, eight flavonols **(7, 8**, **10**, **13**, **14**, **17**, **18**, and **19**) were identified from both species. In addition, four (**12**, **15**, **16**, **20**) were identified from *S. malaccense*, and three from *S. samarangense* (**9**, **11**, **21**). Compounds **7** and **8** were identified as myricetin (**7**) and myricetin-*O*-rhamnoside (**8**) with *m*/*z* $[M-H]^-$ 317.1821 and 463.2279, respectively. Compounds **9**, **10**, **11**, **13**, **15**, **16**, **17,** and **18** were identified in the negative mode as isoquercetin (*m*/*z* $[M-H]^-$ 463.1943), quercetin (*m*/*z* $[M-H]^-$ 301.0468, hyperin (*m*/*z* $[M-H]^-$ 463.1249), isorhamnetin-*O*-glucoside (*m*/*z* $[M-H]^-$ 477.1945), quercitrin (*m*/*z* $[M-H]^-$ 447.2192), kaempferol-*O*-glucoside (*m*/*z* $[M-H]^-$ 447.2192), quercetin 4′-O-glucuronide (*m*/*z* $[M-H]^-$ 477.2255), and mearnsitrin (*m*/*z* $[M-H]^-$ 477.2544). On the other side, compounds **12**, **14**, **19, 20** and **21** were identified in the positive mode as isorhamnetin-*O*-rhamnoside (*m*/*z* $[M+H]^+$ 463.1954), mearnsetin

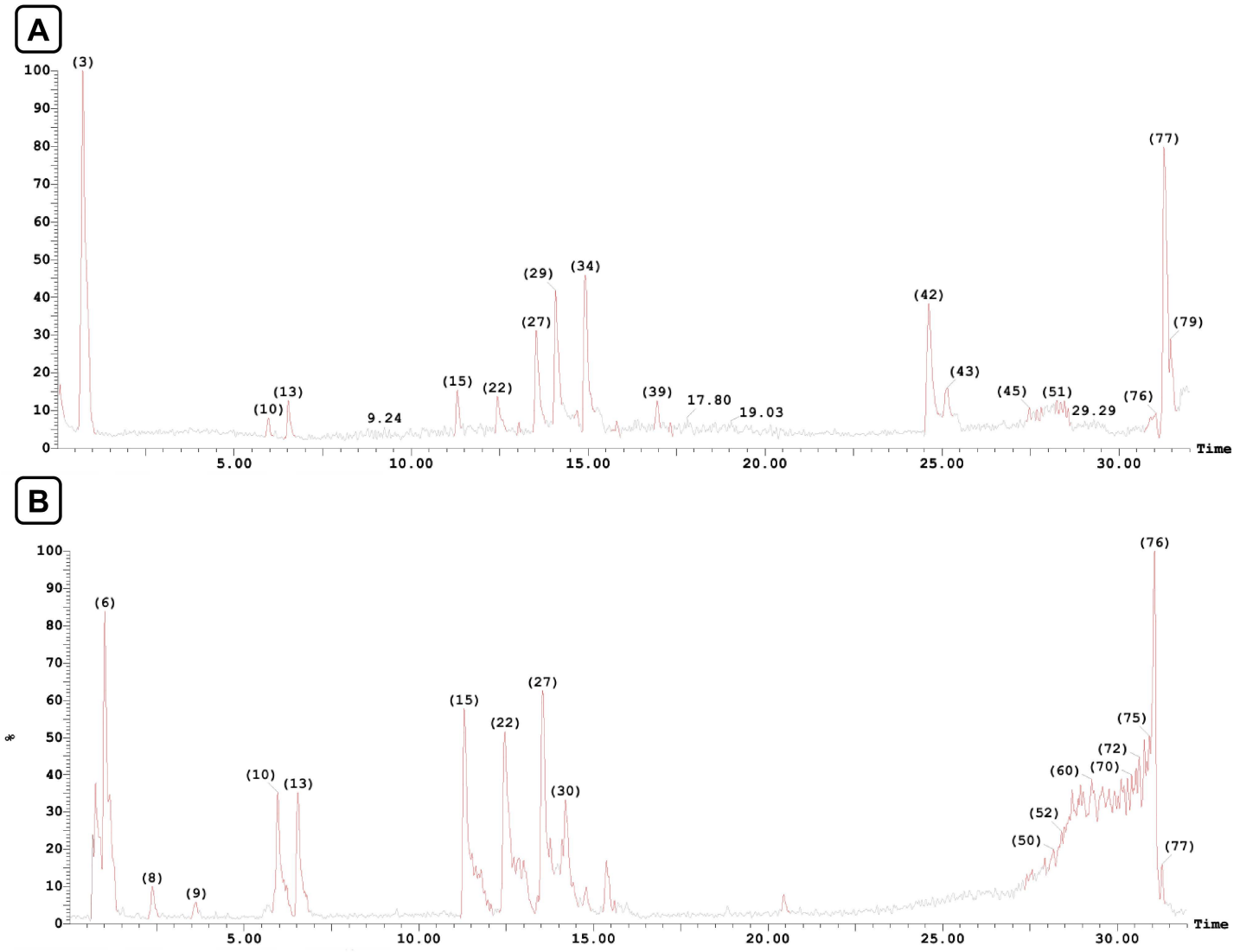

Fig 2. Total ion chromatogram (TIC) obtained from HPLC-MS of the defatted aqueous methanol extract of *S. samarangense* leaves in (A) positive and (B) negative ionization modes.

https://doi.org/10.1371/journal.pone.0329586.g002

(*m*/*z* [M + H]$^+$ 333.11245), kaempferol (*m*/*z* [M + H]$^+$ 287.1558), quercetin 3-*O*-acetyl-galactoside) -*O*-rhamnoside (*m*/*z* [M + H]$^+$ 653.4450) and quercetin 3'-sulfate (*m*/*z* [M + H]$^+$ 383.4042). Compounds **7** (myricetin), **8** (myricetin- *O*-rhamnoside), **10** (quercetin), **14** (mearnsetin), **15** (quercitrin), **18** (mearnsitrin), and **19** (kaempferol) were identified before from *S. malaccense* leaves grown in Brazil but not from the Egyptian species [25,46], while **13 (**isorhamnetin-*O*-glucoside), **16** (kaempferol-*O*-glucoside were identified from its fruits [46]. Flavonols **12** (isorhamnetin-*O*-rhamnoside), **17** (quercetin 4′-*O*-glucuronide), and **20** (quercetin 3-*O*-acetyl-galactoside)-*O*-rhamnoside) were detected for the first time. Ultimately, **compounds 8** (myricetin-*O*-rhamnoside), **9** (isoquercitrin), **10** (quercetin), and **11** (hyperin) were identified before from the leaves of *S. samarangense* grown in Egypt [32,45], compounds **8**, **10**, and **11** were identified from its fruits, while compounds **7** and **19** were detected in its stem bark [36]. Flavonols **7**, **13**, **14**, **17**, **18**, **19**, and **21** were tentatively identified for the first time from *S. samarangense* leaves. Additionally, two flavone glycosides were identified in

the positive mode of *S. malaccense* as diosmin (**23**) (*m*/*z* [M + H]$^+$ 609.4222) and apigenin-7-*O*-diglucuronide (**24**) (*m*/*z* [M + H]$^+$ 623.4117), while 4',7-tetrahydroxyflavone (**22**) (*m*/*z* [M-H]$^-$ 285.1601) was identified in the negative mode of *S. samarangense*. This is the first time to identify the forementioned flavone glycosides from both species, though **22** and **23** were previously detected in other *Syzygium* species [49]. Concerning the flavanone sub-class, eight of them were identified in the analyzed extracts. Pinocembrin **25** (*m*/*z* [M-H]$^-$ 255.1476/ [M + H]$^+$ 257.1037) and cryptostrobin **26** (*m*/*z* [M-H]$^-$ 269.1739/ [M + H]$^+$ 271.0981) were identified in both negative and positive modes of the two species. Naringenin **28** was identified in the positive mode of *S. malaccense* (*m*/*z*[M + H]$^+$ 273.2100) while strobopinin **27** (*m*/*z* [M-H]$^-$ 269.1747), 7-hydroxy-5-methoxy-6,8-
dimethylflavanone **30** (m/z [M-H]$^-$ 297.2050), and 8-prenylnaringenin **31** (m/z [M-H]$^-$ 339.3448) were identified in the negative mode of *S. samarangense.* Additionally, 8-methylpinocembrin **29** (m/z [M + H]$^+$ 271.1037) and 6-geranyl naringenin **32** (*m*/*z*[M + H]$^+$ 409.4701) were identified in its positive mode. This is the first time identifying the flavanones class of metabolites in *S. malaccense,* except naringenin **28,** which was identified before in the Brazilian species [46]. **26** was previously detected in the leaf extract of *S. samarangense* cultivated in Egypt [32], while **25**, **27**, **29**, and **30** were identified from its stem bark [35]. **31** and **32** were identified for the first time from the Egyptian species, while previously reported in other Myrtle species [49]. Skimming the presence of other flavonoid subclasses, three isoflavones were tentatively identified in *S. malaccense.* One of which, namely biochanin A **33** (*m*/*z* [M-H]$^-$ 283.1853/ [M + H]$^+$ 285.1370), is detected in both negative and positive modes. On the other hand, **37** and **38** were identified as pseudobaptigenin (*m*/*z* [M + H]$^+$ 269.1739) and glycitein *m*/*z* [M-H]$^-$ 283.1666), respectively. Moreover, 4'-*O*-methyl equol **33**, dihydrodaidzein **35**, glycitin-6''-*O*-acetate **36,** and genistein 4',7-*O*-diglucuronide **39** were identified in the negative mode of *S. samarangense* with *m*/*z* [M-H]$^-$ 255.1296, 255.1142, 487.4554, and 621.4432, respectively. Interestingly, this is the first report of isoflavones from the two species investigated, but they have been previously detected in other Myrtaceae species [49,50].

Chalcones and their derivatives represent an interesting category of flavonoids due to their versatility and effective bioactivities. They comprise two aromatic rings bridged by an α, β-unsaturated system of three carbons. In this regard, nine **(41–43, 45–47, 49, 50,** and **52)** and twelve **(40, 42–52)** chalcones were identified from *S. malaccense and S. samarangense*, respectively. Chalcones **42**, **43**, **45**, **46**, **47**, **49**, **50**, and **52** were detected in positive and negative modes of both species and elucidated as aurentiacin **42** (*m*/*z* [M-H]$^-$ 297.1133/ [M + H]$^+$ 299.1569), cardamonin **43** (*m*/*z* [M-H]$^-$ 269.1631/ [M + H]$^+$ 271.1143), 2',4'-dihydroxy-6'-methoxy-3'-methyl chalcone **45** (*m*/*z* [M-H]$^-$ 283.1888/ [M + H]$^+$ 285.2387), stercurensin **46** (*m*/*z* [M-H]$^-$ 283.1625/ [M + H]$^+$ 285.1329), demethoxymatteucinol **47** (*m*/*z* [M-H]$^-$ 283.1846/ [M + H]$^+$ 285.1332), 2',4'-dihydroxy-6'-methoxy-3'-methyl dihydrochalcone **49** (*m*/*z* [M-H]$^-$ 285.2119/ [M + H]$^+$ 287.1356), 2′,4′-dihydroxy-6′- methoxy3′,5′- dimethyl dihydrochalcone **50** (*m*/*z* [M-H]$^-$ 297.2200/ [M + H]$^+$ 299.1672) and dimethyl cardamonin **52** (*m*/*z* [M-H]$^-$ 297.2204/ [M + H]$^+$ 299.1618). On the other side, 6,8-di-*C*-methyl pinocembrin-5-methyl ether **41** was detected in the positive mode of *S. malaccense* (*m*/*z* [M + H]$^+$ 299.1618), while phloretin **40**, uvangoletin **44**, 2'-hydroxy-4',6'-dimethoxy chalcone **48** and 4',6'-dihydroxy-3',5'-dimethyl-2'-methoxy chalcone **51** were detected in the negative mode of *S. samarangense* with *m*/*z* [M-H]$^-$ 273.0029, 271.1406, 283.2011 and 297.1987, respectively. Interestingly, this is the first study to report the detection of chalcones in the leaves of *S. malaccense*, while chalcones have been reported before from *S. samarangense.* For instance, **45** was previously identified in *S. samarangense* leaves' extract [51], compounds **42**, **44**, **46**, **47**, **49**, **51,** and **52** were detected in its stem bark [35], and compound **43** from the fruits [52] as well as from other *Syzigium* species [49,51].

Lignin is the most vital and profuse biopolymer that connects cellulose and hemicellulose fibers, providing a rigorous structure to the plant cell [53]. Herein, only one lignin, lariciresinol-sesquilignan **53,** was identified for the first time from the negative mode of *S. malaccense* with (*m*/*z* [M-H]$^-$ 555.4398), but it was previously detected from other Myrtaceae species [49]. Two derivatives were identified for the first time from *S. malaccense*, one of which is 5-heptadecylresorcinol **54** and detected in both ionization modes (*m*/*z* [M-H]$^-$ 347.2201/ [M + H]$^+$349.2050), while the other is adipostatin E **55** and detected in the negative mode only (*m*/*z* [M-H]$^-$ 255.1296). The two compounds were identified earlier from the leaves of *S. samarangense* grown in China [54].

Ultimately, three miscellaneous metabolites were detected for the first time in *S. malaccense* extract and elucidated as malic acid **58** (*m*/*z* [M-H]$^-$ 132.9923), quinic acid **59** (*m*/*z* [M-H]$^-$ 191.1055), and stigmastanol *trans*-ferulate **61 (***m*/*z* [M + H]$^+$ 593.3953). To our knowledge, compounds **58** and **59** were previously identified from *S. samarangense* [32,46]. On the other side, bergapten **56** (*m*/*z* [M-H]$^-$ 215.1005), citric acid **57 (***m*/*z* [M-H]$^-$ 191.0651), 3,5-dimethyl-resveratrol **60** (*m*/*z* [M-H]$^-$ 255.1323), cyanidin 3-*O*-glucosyl-rutinoside **62 (***m*/*z* [M + H]$^+$ 758.7891).

Acute toxicity study

The acute toxicity study was performed to ensure the safe dosing range of the extracts before proceeding to further pharmacological evaluations. Understanding the acute toxicity profile allows the selection of appropriate doses for efficacy studies while minimizing potential adverse effects. Herein, twenty-four hours post-extract administration, no changes were observed in the motor activity or the behavior of the tested animals, and no mortality was recorded. Therefore, both DEs were considered safe till 5 g/kg, and, consequently, we selected dose levels of 250, 500, and 1000 mg/kg to evaluate the extract's nephroprotective effect.

In vivo nephroprotective activity

Effect of the DE of *S. malaccense* and *S. samarangense* on the levels of urea and creatinine. As seen in Table 3, $CdCl_2$ induced kidney tissue damage that affected the function of the glomeruli, evidenced by the significant ($p < 0.001$) increase in the levels of urea and creatinine in $CdCl_2$-treated rats by 4.4-fold and 3.7-fold, respectively, compared to the control group. Both tested extracts preserved the renal function evidenced by the significant ($p < 0.001$) decrease in urea and creatinine levels as follows: DE of *S. malaccense* in doses 250, 500, and 1000 mg/kg significantly declined urea levels by 33.5%, 64.1%, and 69.2%, respectively; and decreased creatinine levels by 22.3%, 52.9%, and 60.6%, respectively, compared to the $CdCl_2$-treated rats. Meanwhile, *S. samarangense* significantly ($p < 0.001$) decreased urea levels by 45.3%, 68.9%, and 70.2%, respectively, and decreased creatinine levels by 25.8%, 61.5%, and 65.4%, respectively, compared to the $CdCl_2$-treated rats.

Effect of the DE of *S. malaccense* and *S. samarangense* leaves on oxidative stress parameters. Oxidative damage induced by $CdCl_2$ is evidenced by the marked ($p < 0.001$) decrease in GSH by 74.6% and SOD by 84.4%, compared to the control group. Doses of 250, 500, and 1000 mg/kg from the DE of *S. malaccense* significantly ($p < 0.001$) boosted the level of GSH by 1.7, 2.7, and 3.3 folds, respectively; and SOD by 2.4, 4.3, and 5 folds, respectively, compared to $CdCl_2$-treated group. Meanwhile, doses of 250, 500, and 1000 mg/kg from *S. samarangense* significantly ($p < 0.001$) enhanced the level of GSH by 1.7, 2.7, and 3.3 folds, respectively. In addition, they potentiated the level of SOD by 2.6, 4.8, and 6.4 folds, respectively, compared to the $CdCl_2$-treated group. These findings support their antioxidant property (Figs 3A and 3B).

Effect of the DE of *S. malaccense* and *S. samarangense* leaves on inflammatory parameters. Inflammation is involved in $CdCl_2$-induced damage, as seen in $CdCl_2$-treated rats. They manifested a marked ($p < 0.001$) elevation in TNF-α, IL-1β, and p-NF-κB p65, by 4.8, 4.0, and 3.5 folds, respectively, compared to the control rats. Treatment with

Table 3. Effect of different doses of the defatted extract (DE) of the leaves of *S. malaccense* and *S. samarangense* on urea and creatinine levels. Data represented as mean±SEM of n = 7, a: significant from the control group at $p < 0.001$, b: significant from the $CdCl_2$ group at $p < 0.001$.

	Control	$CdCl_2$	*S. malaccense*			*S. samarangense*		
			250	500	1000	250	500	1000
Urea (μmol/mL)	6.674 ± 0.33	29.06 ± 0.61 [a]	19.33 ± 0.74 [a,b]	10.44 ± 0.27 [a,b]	8.952 ± 0.13 [a,b]	15.89 ± 0.48 [a,b]	9.017 ± 0.78 [a,b]	8.648 ± 0.31 [a,b]
Creatinine (nmol/mL)	0.4433 ± 0.02	1.630 ± 0.01 [a]	1.266 ± 0.02 [a,b]	0.768 ± 0.03 [a,b]	0.641 ± 0.03 [a,b]	1.209 ± 0.03 [a,b]	0.628 ± 0.01 [a,b]	0.563 ± 0.02 [a,b]

https://doi.org/10.1371/journal.pone.0329586.t003

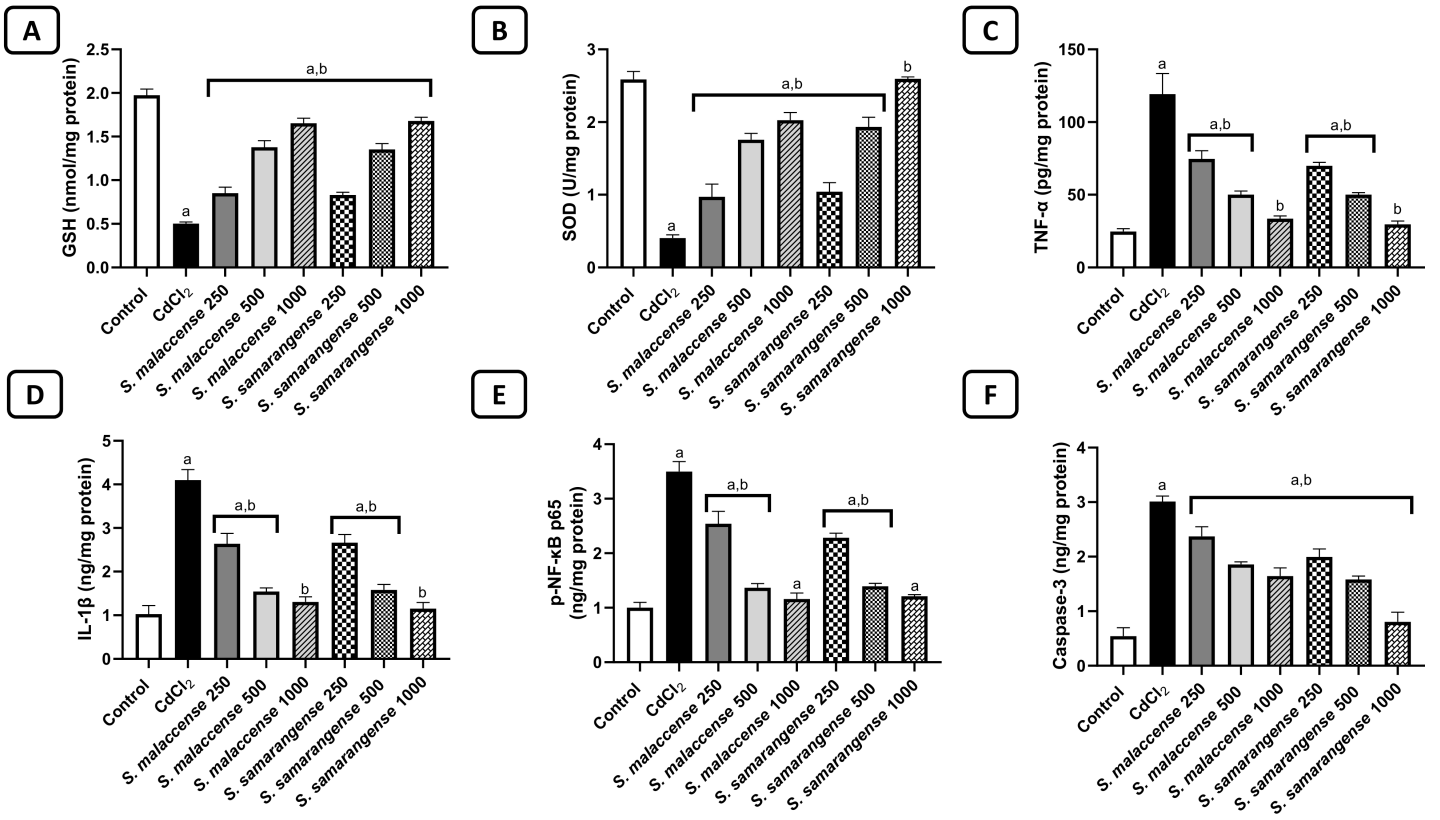

Fig 3. Effect of DE of *S. malaccense* and *S. samarangense* on A) GSH, B) SOD, C) TNF-α, D) IL-1β, E) p-NF-κB, and F) Caspase-3 levels. Data represented as mean±SEM of n = 7. a: significant from the control group at $p < 0.001$, b: significant from the $CdCl_2$ group at $p < 0.001$.

https://doi.org/10.1371/journal.pone.0329586.g003

S. malaccense DE (250, 500, and 1000 mg/kg) significantly ($p < 0.001$) reduced TNF-*α* by 37.4%, 57.9%, and 71.9%; decreased IL-1*β* by 35.6%, 62.4%, and 68.1%; and reduced p-NF-κB p65 by 27.3%, 60.9%, and 66.8%, respectively, compared to the $CdCl_2$-treated rats. Additionally, treatment with *S. samarangense* (250, 500, and 1000 mg/kg) significantly ($p < 0.001$) decreased TNF-*α* by 41.3%, 57.9%, and 75.1%; and reduced IL-1*β* by 34.9%, 61.4%, and 71.9%; and decreased p-NF-κB p65 by 34.7.3%, 60.1%, and 65.4%, respectively, compared to the $CdCl_2$-treated rats. These results indicate the promising anti-inflammatory activity of the tested extracts (Figs 3C-3E).

Effect of the DE of *S. malaccense* and *S. samarangense* leaves on the apoptotic parameter caspase-3. Treatment with $CdCl_2$ induced apoptosis of renal tissue as indicated by the marked ($p < 0.001$) increase in caspase-3 level in $CdCl_2$-treated rats by 5.6-fold compared to the control rats. Meanwhile, administration of *S. malaccense* (250, 500, and 1000 mg/kg) significantly ($p < 0.001$) reduced the caspase-3 level by 21.2%, 38.2%, and 45.4%, respectively, compared to the $CdCl_2$-treated rats. Moreover, treatment with *S. samarangense* (250, 500, and 1000 mg/kg) significantly ($p < 0.001$) decreased the caspase-3 level by 33.8%, 47.5%, and 73.3%, respectively, compared to the $CdCl_2$-treated rats. These results suggest the anti-apoptotic and cytoprotective effect of *S. malaccense* and *S. samarangense* DEs (Fig 3F).

Effect of the DE of *S. malaccense* and *S. samarangense* leaves on the mitochondrial dysfunction parameters. The $CdCl_2$-treated group showed a significant ($p < 0.001$) reduction in ATP by 68.5% compared to the control rats. Groups treated with the DE of *S. malaccense* at doses 250, 500, and 1000 mg/kg showed a marked ($p < 0.001$) increase in ATP by 1.6, 2.7, and 3.2 folds, respectively, compared to the $CdCl_2$-treated group. Additionally, groups

administered the DE of *S. samarangense* at doses 250, 500, and 1000 mg/kg showed a significant ($p < 0.001$) increase in ATP by 1.6, 2.5, and 3.3 folds, respectively, compared to the $CdCl_2$-treated rats (Fig 4A).

Effect of the DE of *S. malaccense* and *S. samarangense* leaves on autophagy parameters. Induction of autophagy was detected by measuring *p*-mTOR and beclin-1. As presented in Figs 4B and 4C, the $CdCl_2$-treated group demonstrated a marked ($p < 0.05$) decrease in *p*-mTOR by 79.6% and a marked ($p < 0.001$) increase in beclin-1 by 2.4-fold compared to the control group. Meanwhile, groups administered with 250, 500, and 1000 mg/kg of *S. malaccense* DE significantly ($p < 0.001$) increased *p*-mTOR by 2, 3.5, and 4.7 folds; and decreased beclin-1 by 12.9%, 43.3%, and 49.5%, respectively, compared to $CdCl_2$-treated groups. Groups treated with 250, 500, and 1000 mg/kg of *S. samarangense* DE significantly ($p < 0.001$) increased *p*-mTOR by 2.3, 3.9, and 4.9 folds; and decreased beclin-1 by 27.8%, 45.4%, and 56.1%, respectively, compared to $CdCl_2$-treated groups. Regarding the level of p-AMPK, the $CdCl_2$-treated group showed a marked ($p < 0.001$) elevation in p-AMPK by 2.1-fold compared to the control group. Groups treated with the DE of *S. malaccense* at doses 250, 500, and 1000 mg/kg showed a significant ($p < 0.001$) decrease in p-AMPK by 22.4%, 43.2%, and 49.2%, respectively, compared to the $CdCl_2$-treated group. Additionally, groups administered the DE of *S.*

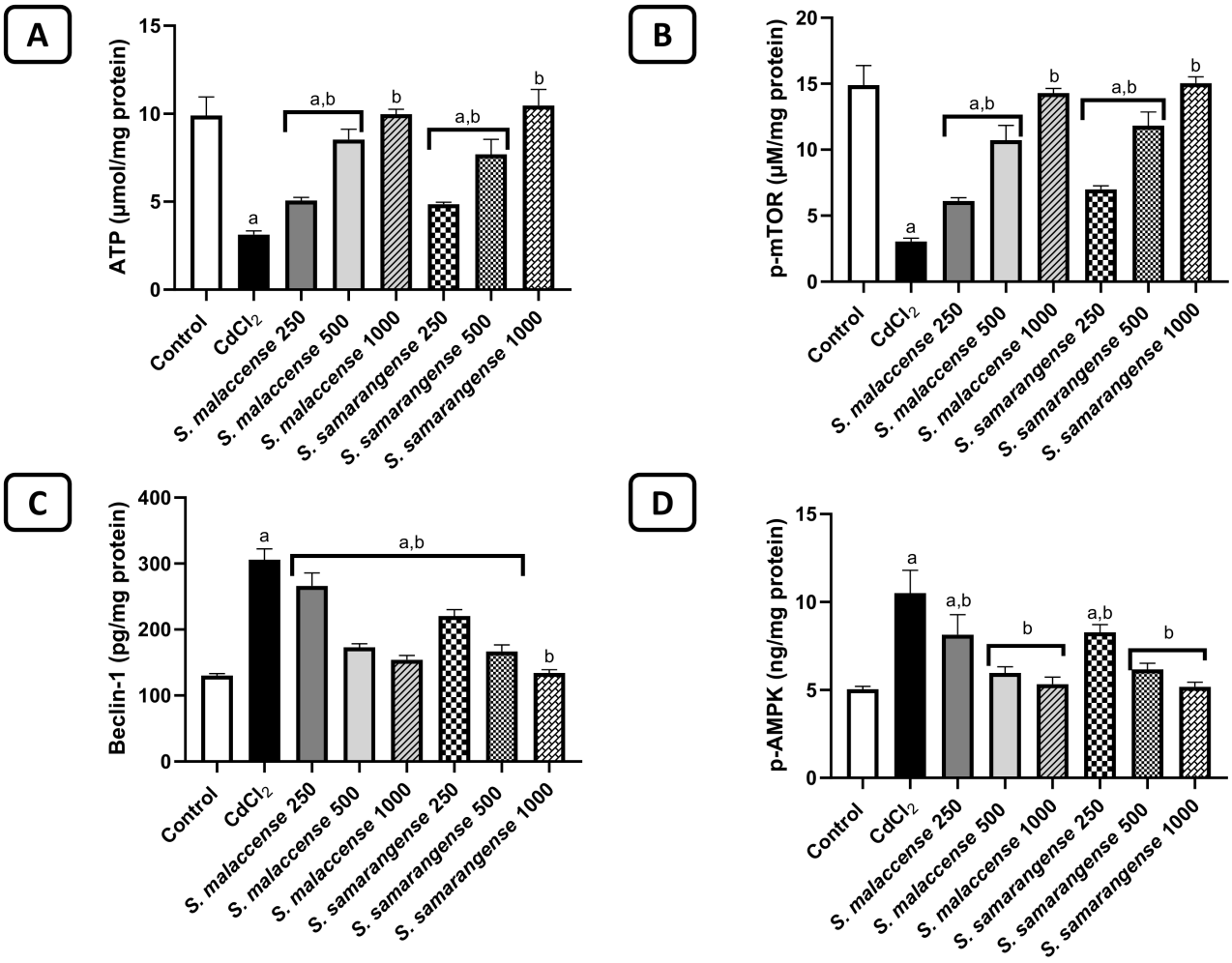

Fig 4. Effect of DE of *S. malaccense* and *S. samarangense* leaves on A) ATP, B) p-mTOR, C) beclin-1, and D) p-AMPK levels. Data represented as mean±SEM of n = 7. a: significant from the control group at $p < 0.001$, b: significant from the $CdCl_2$ group at $p < 0.001$.

https://doi.org/10.1371/journal.pone.0329586.g004

samarangense at doses 250, 500, and 1000 mg/kg showed a marked ($p < 0.001$) decrease in p-AMPK by 21.1%, 41.2%, and 50.6%, respectively, compared to the $CdCl_2$-treated group (Fig 4D).

Effect of the DE of *S. malaccense* and *S. samarangense* on serum ALT and AST levels. As delineated in Table 4, $CdCl_2$-treated rats exhibited a significant elevation in serum ALT and AST levels compared to the control group ($p < 0.001$) by 2.8 and 2.9 folds, respectively, indicating systemic hepatic toxicity. Treatment with the DE of *S. malaccense* at doses 250, 500, and 1000 mg/kg significantly decreased the serum level of ALT by 26.1%, 33.3%, and 57.5%, and AST by 34.9%, 53.4%, and 58.6%, respectively, compared to the $CdCl_2$ group ($p < 0.05$). Meanwhile, treatment with the DE of *S. samarangense* at 250, 500, and 1000 mg/kg significantly decreased the serum level of ALT by 30.5%, 46.8%, and 58.6%, and AST by 35.4%, 56.1%, and 62.0%, respectively, compared to the $CdCl_2$ group ($p < 0.05$). These results suggest a protective effect of the DEs against CdCl2-induced liver injury.

Effect of the DE of *S. malaccense* and *S. samarangense* leaves on histopathological examination of the kidney tissues. As seen in Fig 5, normal kidney samples showed almost intact, well-organized morphological features of renal parenchyma. It showed apparent intact renal tubular segments and intact tubular epithelium (arrow), minimal records of degenerated tubular epithelial cells, intact renal corpuscles (star), and intact vasculatures. However, $CdCl_2$-treated samples showed multiple focal records of periglomerular and perivascular mononuclear inflammatory cell infiltrates accompanied by higher fibroblastic activity (red arrow) with dilatation of renal vasculatures (red star). Both DEs of *S. malaccense* and *S. samarangense* (250 mg/kg) showed mild persistent records of perivascular and periglomerular inflammatory cell infiltrates (red arrow) with almost intact vasculatures and apparent intact nephronal segments. *S. malaccense* at a dose of 500 mg/kg showed higher protective efficacy with a few occasional records of interstitial inflammatory cell infiltrates (red arrow). In comparison, 1000 mg/kg demonstrated higher protective efficacy with almost intact renal parenchyma resembling normal control samples. The 500 mg/kg and 1000 mg/kg of *S. samarangense* showed higher protective efficacy with almost intact renal parenchyma resembling normal control samples.

Discussion

The kidneys are among the most energy-intensive organs, crucial for maintaining water and salt equilibrium [69]. They receive nearly 25% of the cardiac output and are responsible for blood pressure management and continuous blood filtration [70]. Cadmium (Cd) pollution is escalating globally due to heightened industrial operations, which have augmented its availability and environmental persistence. Furthermore, it poses a significant public health hazard owing to its non-biodegradability and extended biological half-life (10–30 years) [71]. Environmental Cd may accumulate in different human organs, including the liver and lungs. However, the kidney is still the main target of its accumulation [72,73], making it mainly susceptible to Cd-mediated nephrotoxicity. Flavonoids are unique, natural bioactive secondary metabolites with a basic flavan skeleton. They comprise two phenyl rings connected to a central heterocyclic pyran scaffold, forming a C6-C3-C6 system with a distinguished polyphenolic feature. Flavonoids are allocated into six major groups, *viz.* flavanols, flavanones, flavonols, flavones, isoflavonoids, and anthocyanidins, in addition to other minor classes including chalcones, dihydrochalcones, and aurones. Flavonoids are found extensively in plant-based meals, so they are ingested through fruits and vegetables [74]. They exhibited beneficial pharmacological effects, including antioxidant, free radical scavenging, anti-inflammatory, immunomodulatory, and renal protective effects [75]. Given the global health burden of Cd toxicity on human health, and the potential therapeutic impacts of polyphenols, especially flavonoids, we investigated the protective potential of two phenolic-rich Syzygium species against cadmium chloride-induced nephrotoxicity in rats. The study showed high serum creatinine and urea levels in Cd-treated rats, indicating kidney injury. The levels of these parameters are usually used as biomarkers for assessing kidney function [76]. According to Gowda et al. [77], urea is a byproduct of the breakdown of proteins and amino acids, and an increase in its blood level is typically linked to renal failure or illness. Another biomarker is creatinine, which is mainly removed by glomerular filtration and created during muscle metabolism from creatine and phosphocreatine. In the current investigation, we reported that the DE of *S. malaccense* and *S.*

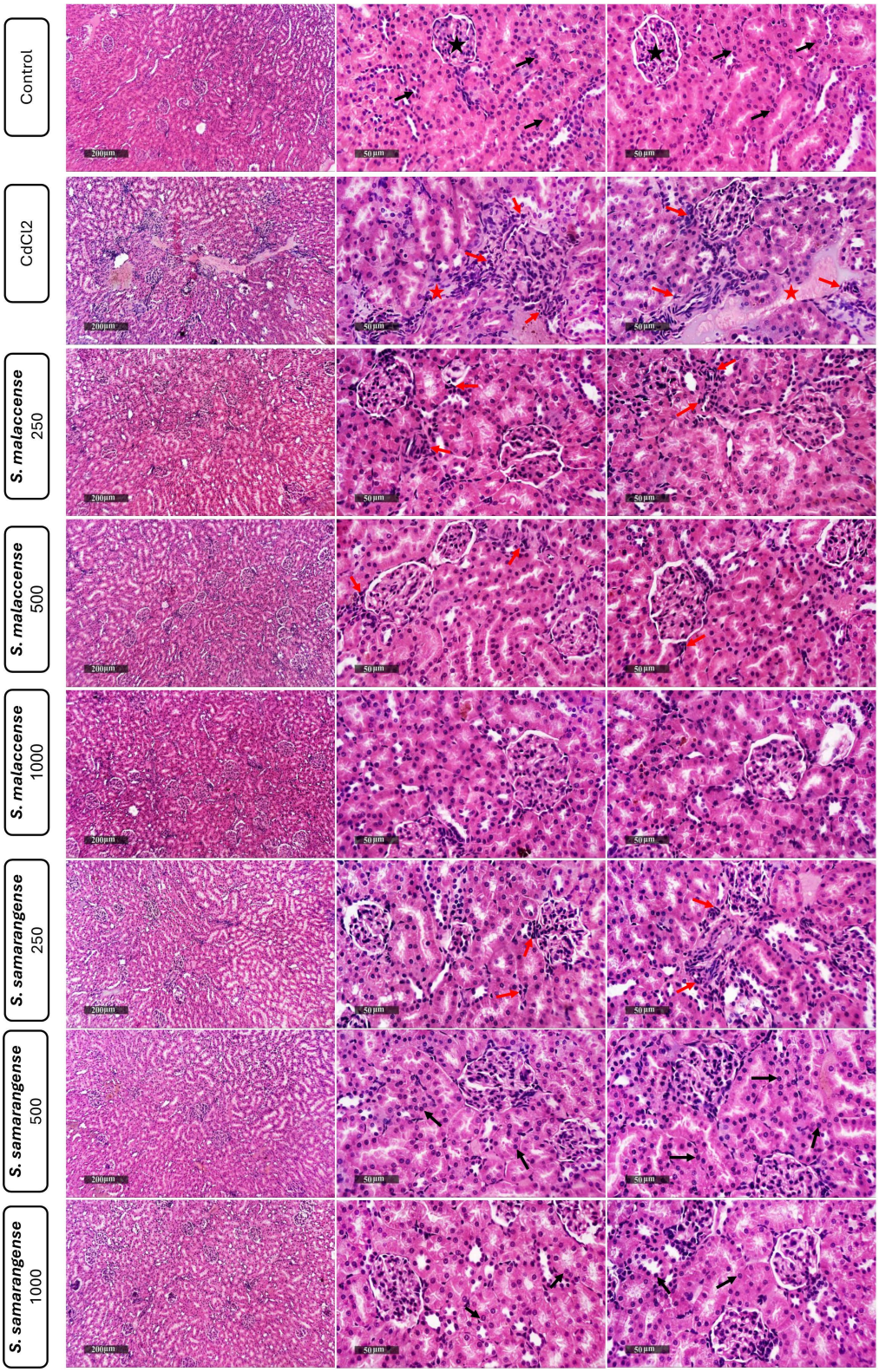

Fig 5. Effect of DE of *S. malaccense* and *S. samarangense* leaves on histopathological examination of the kidney tissues. Normal kidney samples showed intact renal parenchyma with renal tubular segments and intact tubular epithelium (arrow), intact renal corpuscles (star), and intact vasculature. $CdCl_2$-treated samples showed multiple focal periglomerular and perivascular mononuclear inflammatory cell infiltrates accompanied by higher

fibroblastic activity (red arrow) with dilatation of renal vasculatures (red star). DEs of *S. malaccense* and *S. samarangense* at 250 mg/kg doses showed mild perivascular and periglomerular inflammatory cell infiltrates (red arrow) with almost intact vasculatures and nephron segments. *S. malaccense* at a dose of 500 mg/kg showed higher protective efficacy with few occasional interstitial inflammatory cell infiltrates (red arrow). In comparison, the 1000 mg/kg showed higher protective efficacy with almost intact renal parenchyma. 500 mg/kg and 1000 mg/kg of *S. samarangense* showed a higher protective efficacy with almost intact renal parenchyma resembling normal control samples.

https://doi.org/10.1371/journal.pone.0329586.g005

Table 4. Effect of different doses (mg/Kg) of the defatted extract (DE) of the leaves of *S. malaccense* and *S. samarangense* on serum ALT and AST levels. Data represented as mean±SEM of n = 7, a: significant from the control group at $p < 0.001$, b: significant from the $CdCl_2$ group at $p < 0.001$.

	Control	$CdCl_2$	*S. malaccense* (mg/Kg)			*S. samarangense* (mg/Kg)		
			250	500	1000	250	500	1000
ALT (ng/mL)	1.41 ± 0.04	4.08 ± 0.16 [a]	3.02 ± 0.11 [a,b]	2.72 ± 0.09 [a,b]	1.73 ± 0.06 [a,b]	2.84 ± 0.08 [a,b]	2.17 ± 0.07 [a,b]	1.69 ± 0.06 [a,b]
AST (ng/mL)	1.89 ± 0.06	5.55 ± 0.29 [a]	3.61 ± 0.10 [a,b]	2.58 ± 0.11 [a,b]	2.29 ± 0.05 [a,b]	3.58 ± 0.14 [a,b]	2.43 ± 0.12 [a,b]	2.10 ± 0.06 [a,b]

https://doi.org/10.1371/journal.pone.0329586.t004

samarangense reversed Cd-induced nephrotoxicity, evidenced by decreased blood creatinine and urea levels. This finding follows previous reports, which revealed that phenolic compounds improved the nephrotoxicity induced by heavy metals such as Cd [78–80].

Oxidative damage accompanied by free radical overproduction is one of the main processes that are activated upon Cd intoxication. It was established that Cd causes oxidative stress by influencing the pro-to-antioxidant ratio. Additionally, in the biological system, Cd does not undergo redox processes, however, it can generate oxidative stress by intracellular GSH reduction [81], since Cd can bind with the functional thiol (-SH) groups in both enzymatic and non-enzymatic cellular compounds [82]. Moreover, Cd can inhibit other antioxidant enzymes such as SOD which was attributed to the Cd interaction with the enzyme protein part causing a configurational change in the enzyme and results in depressing SOD catalytic activity [83]. The two examined extracts are rich mainly in flavonoids belonging to various classes, exemplified in flavonols **(7−21),** flavone **(22−24),** flavanones **(25–32)**, isoflavones **(33−39)**, and chalcones **(40−52)**. Flavonoids exert their antioxidant effect *via* direct and indirect mechanisms. Directly by donating electrons that neutralize reactive oxygen species (ROS) [84] and free radicals such as peroxynitrite ($ONOO^-$), hydroxyl radical ($OH\cdot$), and peroxyl radical ($ROO\cdot$), hence decreasing ROS and other free radicals levels in the body [85]. Though the sugar part of the flavonoid skeleton is critical for their antioxidant activity, the aglycones are more effective than their corresponding glycosides [86]. On the other hand, the indirect antioxidant effect of flavonoids is associated with inducing the production or activation of antioxidant enzymes and suppressing pro-oxidant enzymes. Flavonoids can activate the intracellular antioxidant signaling pathways to induce the production of intracellular antioxidant elements including GSH and SOD. We cannot neglect the effect of other phenolic classes detected in the two tested DE, such as phenolic acids **(1−6),** resveratrol derivatives (**60**), and lignans (**53**), which are all characterized by their potential antioxidant effect [49,87]. In all, our result revealed that the reduced GSH and SOD levels in the Cd-administrated rats were significantly restored by using the DE of *S. malaccense* and *S. samarangense,* especially at higher doses (500 and 1000 mg/kg). Moreover, several flavonoids and phenolic acids identified in this study were previously reported to have a strong antioxidant effect [33,47,49] and protect against kidney injury [75,87,88]. It is well-known that oxidative stress and inflammation are interrelated processes where elevated levels of ROS enhance NF-κB activation and release of inflammatory cytokines. NF-κB is an essential modulator of the immune system and several inflammatory disorders. Furthermore, it is essential to activate inflammatory cytokines including IL-1β and TNF-α [89]. Prior research has demonstrated that exposure to Cd in renal tissues can trigger the activation of NF-κB, leading to an increase in TNF-*α*, IL-1, and IL-6 [82,90,91]. Our study demonstrated that the examined extracts significantly

decreased the levels of NF-κB, TNF-*α*, and IL-1*β*, especially at higher doses. These results might be attributed to flavonoids, confirmed by earlier reports that disclosed the anti-inflammatory potential of flavonoids and phenolic acids [33,47,49]. Through a variety of processes, including immune cell regulation and enzyme and transcription factor inhibition, flavonoids produce their anti-inflammatory effects. Prior research has demonstrated that flavonoids affect immune cell development, activation, and signaling transduction, which can interfere with cytokine and chemokine synthesis and secretion [47].

Cd-induced oxidative stress and inflammation may trigger apoptosis which has an essential role in Cd-caused nephrotoxicity [92]. Apoptosis results from an imbalance between apoptotic and anti-apoptotic molecules, which is caused by both dependent and independent mitochondrial pathways [5]. Because it can initiate the apoptotic pathway by inducing other caspase enzymes, caspase-3 is considered an essential apoptotic marker [93]. A previous report coincides with our finding that Cd exposure significantly elevates caspase-3 level in the rat's renal tissues [6,94]. In the present study, treatment with our investigated extracts protected against Cd-induced renal apoptosis by inhibiting the activation of caspase-3, which indicates their anti-apoptotic potential against Cd exposure. This effect may be at least in part, due to the extracts' flavonoid and phenolic acids content. Both are renowned for their valuable therapeutic activity on renal health due to their antioxidant, anti-inflammatory, and anti-apoptotic properties [75].

Mitochondria are referred to as the engine of the cell due to their capability to generate ATP via oxidative phosphorylation [95]. They are critical organelles in preserving cellular homeostasis, and therefore, their damage may result in tissue or cellular damage [96]. Renal mitochondrial dysfunction is associated with inflammation, apoptosis, and tissue damage, which raises the risk of death and morbidity [97]. It was documented that Cd exposure decreases the level of ATP because of mitochondrial damage [98], which is consistent with our result. Meanwhile, the level of ATP is increased upon the treatments with the two extracts investigated.

Autophagy is an evolutionary conserved catabolic process used by eukaryotic cells to break down damaged or unnecessary proteins and organelles [99]. It is crucial for the upkeep and survival of cells [100]. It participates in Cd-induced nephrotoxicity [101]. Furthermore, it has been reported to be the early response of a cell to Cd toxicity in a concentration- and time-dependent way [102]. During the early stage of exposure, low levels of Cd may trigger protective autophagy in renal tubular epithelial cells [103–105], but with continuous exposure, excessive autophagy ultimately fails to maintain cell viability and then triggers cell death [7]. Autophagy can result from the activation of many signaling pathways by cellular proteins and/or protein kinases [106]. Amongst them, the AMPK/mTOR is the most significant pathway in autophagy regulation [107]. AMPK usually motivates autophagy by impairing mTOR, which plays an important role in monitoring cell growth, proliferation, and autophagy [108]. Moreover, beclin-1 controls autophagy membrane biosynthesis as it is necessary to initiate autophagosome formation [109]. It was reported that Cd exposure significantly decreases mTOR levels, activates the AMPK, and increases protein levels of beclin-1 [110], which is consistent with our results. Meanwhile, our results showed that the administration of both DEs significantly suppressed the excessive autophagy process, evidenced by decreased levels of AMPK and beclin-1 and increased levels of mTOR. The suppressed autophagy effect of the extracts can be elucidated by their antioxidant, anti-inflammatory, antiapoptotic, and cytoprotective activities.

Histopathological analysis of the kidney tissues showed that Cd caused numerous pathological lesions characterized by inflammatory cell infiltration and vascular dilatation. Additionally, the usual histological features of the renal tubules were lost. Cd exposure results in multiple focal records of periglomerular and perivascular mononuclear inflammatory cell infiltrates accompanied by higher fibroblastic activity with dilatation of renal vasculatures. These histomorphological alterations may be due to the direct damage of the renal tissues and increased ROS generation brought on by exposure to Cd [111]. Hence, resulted in oxidative damage [112] and morphological changes in renal tissue. However, the *S. malaccense* and *S. samarangense* DEs, especially at higher doses, display potential protective effects on the kidney tissues, which may be related to the strong antioxidant potential of flavonoids. Flavonoids significantly attenuated the oxidative stress, causing a decrease in pathological changes [49,87].

Cd is well-documented to induce not only nephrotoxicity but also systemic toxicity, particularly hepatotoxicity, through oxidative stress and mitochondrial dysfunction [113,114]. Elevated ALT and AST levels have been observed in the $CdCl_2$ group, confirming hepatic injury. The ability of the DE of *S. malaccense* and *S. samarangense* to reduce these liver enzyme levels suggests a broader systemic protective role, possibly *via* antioxidant or anti-inflammatory effects.

Conclusion

The current research reported that the defatted aqueous methanol extracts (DE) of *S. malaccense* and *S. samarangense* leaves are rich in various classes of flavonoids, such as flavonols, flavone, flavanones, isoflavones, and chalcones, in addition to other phenolic compounds. The administration of the two investigated extracts significantly attenuated Cd-induced renal toxicity by fighting renal oxidative stress, apoptosis, and inflammatory reactions. Moreover, the two extracts alleviated mitochondrial dysfunction and inhibited the autophagy level in a dose-dependent manner. The nephroprotective effects of the two *Syzygium* extracts against Cd-induced nephrotoxicity may be attributed to anti-inflammatory, antiapoptotic, and antioxidant activities of their constitutive phenolic metabolites. Moreover, the DE not only protects renal function but also mitigates systemic Cd-induced hepatic toxicity. However, implementing *in vitro* experiments using renal cell lines and setting quality control parameters for the HPLC-MS are among the study limitations. In all, the two *Syzygium* extracts can be used, at least in part, as a protective agent against environmental toxicity by heavy metals such as cadmium. Nevertheless, future clinical studies are required to test their toxicity and curing ability for Cd-induced renal dysfunctions in humans. Furthermore, formulating these extracts into a suitable pharmaceutical preparation will facilitate their usage as protective nutraceuticals for kidney nephrotoxicity.

Studies in animal statements

The Faculty of Pharmacy's Ethical Animal Care and Use Committee approved the experimental protocol at Helwan University (approval number: 11A2023). The animal experiment complied with ARRIVE (Animal Research: Reporting of *In Vivo* Experiments) guidelines. Also, it followed the guidance on the operation of the Animals (Scientific Procedures) Act 1986, the association guidelines, EU directive 2010/63 for the protection of animals used for scientific purposes, the NIH (National Research Council) Guide for the Care and Use of Laboratory Animals (8^{th} edition), and national guidelines for animal care (European Community Directive, 6/609/EEC).

Supporting information

S1 Checklist. Humane endpoints checklist. This checklist details the implementation of humane endpoints in the animal experiment described in the study. It includes information on monitoring criteria, euthanasia timing, animal welfare considerations, and compliance with ethical standards, as per PLOS ONE and ARRIVE guidelines.
(DOCX)

Author contributions

Conceptualization: Fatma A. Moharram, Samah Shabana, Heba E. Elsayed.

Data curation: Sahar S. Salem, Samah Shabana, Elsayed K. El-Sayed, Shimaa K. Mohamed, Mohamed A. Khattab, Asmaa A. Ahmed, Heba E. Elsayed.

Formal analysis: Fatma A. Moharram, Samah Shabana, Elsayed K. El-Sayed, Shimaa K. Mohamed, Mohamed A. Khattab, Kuei-Hung Lai, Asmaa A. Ahmed, Heba E. Elsayed.

Funding acquisition: Kuei-Hung Lai.

Investigation: Fatma A. Moharram, Samah Shabana, Elsayed K. El-Sayed, Shimaa K. Mohamed, Mohamed A. Khattab, Asmaa A. Ahmed, Heba E. Elsayed.

Methodology: Fatma A. Moharram, Sahar S. Salem, Samah Shabana, Elsayed K. El-Sayed, Shimaa K. Mohamed, Mohamed A. Khattab, Asmaa A. Ahmed, Heba E. Elsayed.

Resources: Fatma A. Moharram, Samah Shabana, Kuei-Hung Lai.

Supervision: Fatma A. Moharram, Samah Shabana, Heba E. Elsayed.

Writing – original draft: Fatma A. Moharram, Sahar S. Salem, Samah Shabana, Elsayed K. El-Sayed, Shimaa K. Mohamed, Mohamed A. Khattab, Kuei-Hung Lai, Asmaa A. Ahmed, Heba E. Elsayed.

Writing – review & editing: Fatma A. Moharram, Samah Shabana, Elsayed K. El-Sayed, Shimaa K. Mohamed, Mohamed A. Khattab, Kuei-Hung Lai, Asmaa A. Ahmed, Heba E. Elsayed.

References

1. Badawy S, Abd-Elraouf M, Gab-Allah MS, El-Mashad ABI, Tantawy AA, Amin AA. Nephroprotective properties of palm dates and olive leaves extracts on cadmium-induced acute renal toxicity in albino rats. J Advance Vet Res. 2023;13(8):1497–506.
2. Mezynska M, Brzóska MM. Environmental exposure to cadmium-a risk for health of the general population in industrialized countries and preventive strategies. Environ Sci Pollut Res Int. 2018;25(4):3211–32. https://doi.org/10.1007/s11356-017-0827-z PMID: 29230653
3. Negm SH, El-Soadaa SS. Effect of Terminalia chebula on cadmium-induced nephrotoxicity and lipid profiles in rats. Biosci Res. 2020;17:1535–44.
4. Erboga M, Kanter M, Aktas C, Sener U, Fidanol Erboga Z, Bozdemir Donmez Y, et al. Thymoquinone Ameliorates Cadmium-Induced Nephrotoxicity, Apoptosis, and Oxidative Stress in Rats is Based on its Anti-Apoptotic and Anti-Oxidant Properties. Biol Trace Elem Res. 2016;170(1):165–72. https://doi.org/10.1007/s12011-015-0453-x PMID: 26226832
5. Sinha K, Das J, Pal PB, Sil PC. Oxidative stress: the mitochondria-dependent and mitochondria-independent pathways of apoptosis. Arch Toxicol. 2013;87(7):1157–80. https://doi.org/10.1007/s00204-013-1034-4 PMID: 23543009
6. Algefare AI. Renoprotective and Oxidative Stress-Modulating Effects of Taxifolin against Cadmium-Induced Nephrotoxicity in Mice. Life (Basel). 2022;12(8):1150. https://doi.org/10.3390/life12081150 PMID: 36013329
7. Chargui A, Zekri S, Jacquillet G, Rubera I, Ilie M, Belaid A, et al. Cadmium-induced autophagy in rat kidney: an early biomarker of subtoxic exposure. Toxicol Sci. 2011;121(1):31–42. https://doi.org/10.1093/toxsci/kfr031 PMID: 21325019
8. Gong Z-G, Zhao Y, Wang Z-Y, Fan R-F, Liu Z-P, Wang L. Epigenetic regulator BRD4 is involved in cadmium-induced acute kidney injury via contributing to lysosomal dysfunction, autophagy blockade and oxidative stress. J Hazard Mater. 2022;423(Pt A):127110. https://doi.org/10.1016/j.jhazmat.2021.127110 PMID: 34523489
9. Elkhadragy MF, Al-Olayan EM, Al-Amiery AA, Abdel Moneim AE. Protective Effects of Fragaria ananassa Extract Against Cadmium Chloride-Induced Acute Renal Toxicity in Rats. Biol Trace Elem Res. 2018;181(2):378–87. https://doi.org/10.1007/s12011-017-1062-7 PMID: 28567583
10. Liu W, Cui X, Zhong Y, Ma R, Liu B, Xia Y. Phenolic metabolites as therapeutic in inflammation and neoplasms: Molecular pathways explaining their efficacy. Pharmacol Res. 2023;193:106812. https://doi.org/10.1016/j.phrs.2023.106812 PMID: 37271425
11. Sun W, Shahrajabian MH. Therapeutic Potential of Phenolic Compounds in Medicinal Plants-Natural Health Products for Human Health. Molecules. 2023;28(4):1845. https://doi.org/10.3390/molecules28041845 PMID: 36838831
12. Nurzyńska-Wierdak R. Phenolic Compounds from New Natural Sources-Plant Genotype and Ontogenetic Variation. Molecules. 2023;28(4):1731. https://doi.org/10.3390/molecules28041731 PMID: 36838719
13. Hefer M, Huskic IM, Petrovic A, Raguz-Lucic N, Kizivat T, Gjoni D, et al. A mechanistic insight into beneficial effects of polyphenols in the prevention and treatment of nephrolithiasis: evidence from recent *in vitro* studies. Crystals. 2023;13(7):1070. https://doi.org/10.3390/cryst13071070
14. Pandey KB, Rizvi SI. Plant polyphenols as dietary antioxidants in human health and disease. Oxid Med Cell Longev. 2009;2(5):270–8. https://doi.org/10.4161/oxim.2.5.9498 PMID: 20716914
15. Vagkopoulou A, Haddad N, Kontogiorgos I, Papatolios T, Papadopoulou E, Makridis D, et al. #3813 effect of oral flavonoids on arterial stiffness in ckd: a pilot prospective study. Nephrology Dialysis Transplantation. 2023;38(Supplement_1). https://doi.org/10.1093/ndt/gfad063d_3813
16. Haddad N, Bagopoulou N, Kontogiorgos I, Papatolios T, Papadopoulou E, Makridis D, et al. Effect of oral flavonoids on arterial stiffness in ckd – a pilot prospective study. Journal of Hypertension. 2023;41(Suppl 3):e262. https://doi.org/10.1097/01.hjh.0000941692.56078.cc
17. Supriyadi R, Koswara MIA, Soelaeman MA, Huang I. The effect of antioxidants supplementation on oxidative stress and proinflammatory biomarkers in patients with chronic kidney disease: a systematic review and meta-analysis. Eur Rev Med Pharmacol Sci. 2023;27(4):1413–26. https://doi.org/10.26355/eurrev_202302_31379 PMID: 36876681
18. Avila-Carrasco L, García-Mayorga EA, Díaz-Avila DL, Garza-Veloz I, Martinez-Fierro ML, González-Mateo GT. Potential Therapeutic Effects of Natural Plant Compounds in Kidney Disease. Molecules. 2021;26(20):6096. https://doi.org/10.3390/molecules26206096 PMID: 34684678
19. Nayak SS, Bhaijamal RA, Vaghasia J, R S. Role of plant based natural antioxidents on chronic kidney disease. Nat J Pharm Sci. 2023;3(1):101–6. https://doi.org/10.22271/27889262.2023.v3.i1b.74

20. Sujana PKW, Wijayanti N. Phytochemical and antioxidant properties of *Syzygium zollingerianum* leaves extract. Biodiversitas. 2022;23(2). https://doi.org/10.13057/biodiv/d230233
21. Uddin ABMN, Hossain F, Reza ASMA, Nasrin MS, Alam AHMK. Traditional uses, pharmacological activities, and phytochemical constituents of the genus *Syzygium*: A review. Food Sci Nutr. 2022;10(6):1789–819. https://doi.org/10.1002/fsn3.2797 PMID: 35702283
22. Ahmad B, Baider C, Bernardini B, Biffin E, Brambach F, Burslem D, et al. *Syzygium* (Myrtaceae): Monographing a taxonomic giant via 22 coordinated regional revisions. PeerJ. 2016. https://doi.org/10.7287/peerj.preprints.1930v1
23. -Syzygium Working Group. *Syzygium* (Myrtaceae): Monographing a taxonomic giant via 22 coordinated regional revisions. Peer Journal Preprints. 2016. https://peerj.com/preprints/1930.pdf.
24. Panggabean G. *Syzygium malaccense* (L.) Merr. & Perry. In: Verheij EWM, Coronel RE. Bogor, Indonesia: PROSEA Foundation. 1991.
25. Batista ÂG, da Silva JK, Betim Cazarin CB, Biasoto ACT, Sawaya ACHF, Prado MA, et al. Red-jambo (*Syzygium malaccense*): Bioactive compounds in fruits and leaves. LWT - Food Science and Technology. 2017;76:284–91. https://doi.org/10.1016/j.lwt.2016.05.013
26. Dunstan CA, Noreen Y, Serrano G, Cox PA, Perera P, Bohlin L. Evaluation of some Samoan and Peruvian medicinal plants by prostaglandin biosynthesis and rat ear oedema assays. J Ethnopharmacol. 1997;57(1):35–56. https://doi.org/10.1016/s0378-8741(97)00043-3 PMID: 9234163
27. Noreen Y, Serrano G, Perera P, Bohlin L. Flavan-3-ols isolated from some medicinal plants inhibiting COX-1 and COX-2 catalysed prostaglandin biosynthesis. Planta Med. 1998;64(6):520–4. https://doi.org/10.1055/s-2006-957506 PMID: 9741297
28. Prasniewski A, da Silva C, Ayres BRB, da Silva EA, Pilau EJ, Nani BD, et al. Characterization of phenolic compounds by UHPLC-QTOF-MS/MS and functional properties of *Syzygium malaccense* leaves. South African Journal of Botany. 2021;139:418–26. https://doi.org/10.1016/j.sajb.2021.01.036
29. Batista ÂG, da Silva-Maia JK, Júnior MRM. Bioactive Compounds of Red-Jambo Fruit (*Syzygium malaccense* (L.) Merr. & L.M. Perry). Reference Series in Phytochemistry. Springer International Publishing. 2020. 395–407. https://doi.org/10.1007/978-3-030-30182-8_27
30. Savi A, Calegari MA, Calegari GC, Santos VAQ, Wermuth D, da Cunha MAA, et al. Bioactive compounds from *Syzygium malaccense* leaves: optimization of the extraction process, biological and chemical characterization. Acta Sci Technol. 2020;42:e46773. https://doi.org/10.4025/actascitechnol.v42i1.46773
31. Mukaromah AS. Wax Apple (*Syzygium samarangense* (Blume) Merr. & L.M. Perry): A Comprehensive Review in Phytochemical and Physiological Perspectives. AH. 2020;3(1):40–58. https://doi.org/10.21580/ah.v3i1.6070
32. Sobeh M, Youssef FS, Esmat A, Petruk G, El-Khatib AH, Monti DM, et al. High resolution UPLC-MS/MS profiling of polyphenolics in the methanol extract of *Syzygium samarangense* leaves and its hepatoprotective activity in rats with CCl4-induced hepatic damage. Food Chem Toxicol. 2018;113:145–53. https://doi.org/10.1016/j.fct.2018.01.031 PMID: 29374594
33. Nair AGR, Krishnan S, Ravikrishna C, Madhusudanan KP. New and rare flavonol glycosides from leaves of *Syzygium samarangense*. Fitoterapia. 1999;70(2):148–51. https://doi.org/10.1016/s0367-326x(99)00013-1
34. *Syzygium Samarangense*: Review of Phytochemical Compounds and Pharmacological Activities. Biointerface Res Appl Chem. 2022;12(2):2084–107. https://doi.org/10.33263/briac122.20842107
35. LC-MS Chemical Profiling of Dichloromethane Fraction of Methanol Extract of *Syzygium sam*arangense Stem Bark. TJNPR. 2024;8(4):6963–74. https://doi.org/10.26538/tjnpr/v8i4.30
36. Wolfender J-L, Rodriguez S, Hostettmann K. Liquid chromatography coupled to mass spectrometry and nuclear magnetic resonance spectroscopy for the screening of plant constituents. Journal of Chromatography A. 1998;794(1–2):299–316. https://doi.org/10.1016/s0021-9673(97)00939-4
37. Yang M, Sun J, Lu Z, Chen G, Guan S, Liu X, et al. Phytochemical analysis of traditional Chinese medicine using liquid chromatography coupled with mass spectrometry. J Chromatogr A. 2009;1216(11):2045–62. https://doi.org/10.1016/j.chroma.2008.08.097 PMID: 18804769
38. Zilic S, Serpen A, Akillioglu G, Jankovic M, Gokmen V. Distributions of phenolic compounds, yellow pigments, and oxidative enzymes in wheat grains and their relation to antioxidant capacity of bran and debranned flour. J Cereal Sci. 2012;56:652–8. https://doi.org/10.1016/j.jcs.2012.07.014
39. Ansari MN, Rehman NU, Karim A, Imam F, Hamad AM. Protective Effect of *Thymus serrulatus* Essential Oil on Cadmium-Induced Nephrotoxicity in Rats, through Suppression of Oxidative Stress and Downregulation of NF-κB, iNOS, and Smad2 mRNA Expression. Molecules. 2021;26(5):1252. https://doi.org/10.3390/molecules26051252 PMID: 33652584
40. Soliman HSM, Korany EM, El-Sayed EK, Aboelyazed AM, Ibrahim HA. Nephroprotective effect of *Physalis peruviana* L. calyx extract and its butanolic fraction against cadmium chloride toxicity in rats and molecular docking of isolated compounds. BMC Complement Med Ther. 2023;23(1):21. https://doi.org/10.1186/s12906-023-03845-9 PMID: 36707799
41. Culling CF. Handbook of histopathological and histochemical techniques. 3 ed. Culling CF. London, UK: Butterworths. 2013.
42. Ali A, Wu H, Ponnampalam EN, Cottrell JJ, Dunshea FR, Suleria HAR. Comprehensive Profiling of Most Widely Used Spices for Their Phenolic Compounds through LC-ESI-QTOF-MS^2 and Their Antioxidant Potential. Antioxidants (Basel). 2021;10(5):721. https://doi.org/10.3390/antiox10050721 PMID: 34064351
43. Mani JS, Johnson JB, Hosking H, Ashwath N, Walsh KB, Neilsen PM, et al. Antioxidative and therapeutic potential of selected Australian plants: A review. J Ethnopharmacol. 2021;268:113580. https://doi.org/10.1016/j.jep.2020.113580 PMID: 33189842

44. Ali AM, Gabbar MA, Abdel-Twab SM, Fahmy EM, Ebaid H, Alhazza IM, et al. Antidiabetic Potency, Antioxidant Effects, and Mode of Actions of *Citrus reticulata* Fruit Peel Hydroethanolic Extract, Hesperidin, and Quercetin in Nicotinamide/Streptozotocin-Induced Wistar Diabetic Rats. Oxid Med Cell Longev. 2020;2020:1730492. https://doi.org/10.1155/2020/1730492 PMID: 32655759

45. El-Sayed EK, Tawfik N. Phytochemical profile and analgesic activity for two *Syzygium* species. J Adv Pharm Res. 2024;8(1):21–8. https://doi.org/10.21608/aprh.2024.255361

46. Prasniewski A, da Silva C, Ayres BRB, da Silva EA, Pilau EJ, Nani BD, et al. Characterization of phenolic compounds by UHPLC-QTOF-MS/MS and functional properties of *Syzygium malaccense* leaves. South African Journal of Botany. 2021;139:418–26. https://doi.org/10.1016/j.sajb.2021.01.036

47. Cao Y-L, Lin J-H, Hammes H-P, Zhang C. Flavonoids in Treatment of Chronic Kidney Disease. Molecules. 2022;27(7):2365. https://doi.org/10.3390/molecules27072365 PMID: 35408760

48. Corradini E, Foglia P, Giansanti P, Gubbiotti R, Samperi R, Lagana A. Flavonoids: chemical properties and analytical methodologies of identification and quantitation in foods and plants. Nat Prod Res. 2011;25(5):469–95. https://doi.org/10.1080/14786419.2010.482054 PMID: 21391112

49. Ali A, Mueed A, Cottrell JJ, Dunshea FR. LC-ESI-QTOF-MS/MS Identification and Characterization of Phenolic Compounds from Leaves of Australian Myrtles and Their Antioxidant Activities. Molecules. 2024;29(10):2259. https://doi.org/10.3390/molecules29102259 PMID: 38792121

50. Lapčík O, Klejdus B, Kokoška L, Davidová M, Afandi K, Kubáň V, et al. Identification of isoflavones in *Acca sellowiana* and two *Psidium* species (Myrtaceae). Biochemical Systematics and Ecology. 2005;33(10):983–92. https://doi.org/10.1016/j.bse.2005.03.007

51. Amor EC, Villaseñor IM, Nawaz SA, Hussain MS, Choudhary MI. A dihydrochalcone from *Syzygium samarangense* with anticholinesterase activity. Philipp J Sci. 2005;134(2):105–11.

52. Simirgiotis MJ, Adachi S, To S, Yang H, Reynertson KA, Basile MJ, et al. Cytotoxic chalcones and antioxidants from the fruits of a *Syzygium samarangense* (Wax Jambu). Food Chem. 2008;107(2):813–9. https://doi.org/10.1016/j.foodchem.2007.08.086 PMID: 22359426

53. Liu Q, Luo L, Zheng L. Lignins: Biosynthesis and Biological Functions in Plants. Int J Mol Sci. 2018;19(2):335. https://doi.org/10.3390/ijms19020335 PMID: 29364145

54. Hu Y-K, Wang L, Wang J-H, Li M-J, Li F, Yang J, et al. Resorcinol derivatives with α-glucosidase inhibitory activities from *Syzygium samarangense*. Nat Prod Res. 2021;35(24):5948–53. https://doi.org/10.1080/14786419.2020.1805606 PMID: 32787570

55. Rummun N, Pires E, McCullagh J, Claridge TWD, Bahorun T, Li W-W, et al. Methyl gallate – Rich fraction of *Syzygium coriaceum* leaf extract induced cancer cell cytotoxicity via oxidative stress. South African Journal of Botany. 2021;137:149–58. https://doi.org/10.1016/j.sajb.2020.10.014

56. Rocchetti G, Lucini L, Ahmed SR, Saber FR. *In vitro* cytotoxic activity of six Syzygium leaf extracts as related to their phenolic profiles: An untargeted UHPLC-QTOF-MS approach. Food Res Int. 2019;126:108715. https://doi.org/10.1016/j.foodres.2019.108715 PMID: 31732075

57. Soleh Ismail A, Rizal Y, Armenia A, Kasim A. Identification of bioactive compounds in gambier (*Uncaria gambir*) liquid by-product in West Sumatra, Indonesia. Biodiversitas. 2021;22(3). https://doi.org/10.13057/biodiv/d220351

58. Nguyen P-D, Hérent M-F, Le T-B, Bui T-B-H, Bui T-B-H, Do T-T-H, et al. Isolation of quercetin-3-O-sulfate and quantification of major compounds from *Psidium guajava* L. from Vietnam. Journal of Food Composition and Analysis. 2023;115:104928. https://doi.org/10.1016/j.jfca.2022.104928

59. Rehecho S, Hidalgo O, García-Iñiguez de Cirano M, Navarro I, Astiasarán I, Ansorena D, et al. Chemical composition, mineral content and antioxidant activity of Verbena officinalis L. LWT - Food Science and Technology. 2011;44(4):875–82. https://doi.org/10.1016/j.lwt.2010.11.035

60. Stevens JF, Taylor AW, Deinzer ML. Quantitative analysis of xanthohumol and related prenylflavonoids in hops and beer by liquid chromatography-tandem mass spectrometry. J Chromatogr A. 1999;832(1–2):97–107. https://doi.org/10.1016/s0021-9673(98)01001-2 PMID: 10070768

61. Wu Q, Wang M, Simon JE. Determination of isoflavones in red clover and related species by high-performance liquid chromatography combined with ultraviolet and mass spectrometric detection. J Chromatogr A. 2003;1016(2):195–209. https://doi.org/10.1016/j.chroma.2003.08.001 PMID: 14601839

62. Hosoda K, Furuta T, Yokokawa A, Ishii K. Identification and quantification of daidzein-7-glucuronide-4'-sulfate, genistein-7-glucuronide-4'-sulfate and genistein-4',7-diglucuronide as major metabolites in human plasma after administration of kinako. Anal Bioanal Chem. 2010;397(4):1563–72. https://doi.org/10.1007/s00216-010-3714-8 PMID: 20437034

63. Utama K, Khamto N, Meepowpan P, Aobchey P, Kantapan J, Sringarm K, et al. Effects of 2',4'-Dihydroxy-6'-methoxy-3',5'-dimethylchalcone from *Syzygium nervosum* Seeds on Antiproliferative, DNA Damage, Cell Cycle Arrest, and Apoptosis in Human Cervical Cancer Cell Lines. Molecules. 2022;27(4):1154. https://doi.org/10.3390/molecules27041154 PMID: 35208945

64. Memon AH, Ismail Z, Aisha AFA, Al-Suede FSR, Hamil MSR, Hashim S, et al. Isolation, Characterization, Crystal Structure Elucidation, and Anticancer Study of Dimethyl Cardamonin, Isolated from *Syzygium campanulatum* Korth. Evid Based Complement Alternat Med. 2014;2014:470179. https://doi.org/10.1155/2014/470179 PMID: 25530783

65. Singh T, Yadav R, Agrawal V. Effective protocol for isolation and marked enhancement of psoralen, daidzein and genistein in the cotyledon callus cultures of *Cullen corylifolium* (L.) Medik. Industrial Crops and Products. 2019;143:111905. https://doi.org/10.1016/j.indcrop.2019.111905

66. Kosuru R, Rai U, Prakash S, Singh A, Singh S. Promising therapeutic potential of pterostilbene and its mechanistic insight based on preclinical evidence. Eur J Pharmacol. 2016;789:229–43. https://doi.org/10.1016/j.ejphar.2016.07.046 PMID: 27475678

67. Akihisa T, Yasukawa K, Yamaura M, Ukiya M, Kimura Y, Shimizu N, et al. Triterpene alcohol and sterol ferulates from rice bran and their anti-inflammatory effects. J Agric Food Chem. 2000;48(6):2313–9. https://doi.org/10.1021/jf000135o PMID: 10888543

68. Wojdyło A, Nowicka P, Teleszko M. Degradation Kinetics of Anthocyanins in Sour Cherry Cloudy Juices at Different Storage Temperature. Processes. 2019;7(6):367. https://doi.org/10.3390/pr7060367
69. Vart P, Grams ME. Measuring and Assessing Kidney Function. Semin Nephrol. 2016;36(4):262–72. https://doi.org/10.1016/j.semnephrol.2016.05.003 PMID: 27475657
70. Den Hartogh DJ, Tsiani E. Health Benefits of Resveratrol in Kidney Disease: Evidence from In Vitro and In Vivo Studies. Nutrients. 2019;11(7):1624. https://doi.org/10.3390/nu11071624 PMID: 31319485
71. Yang Q, Hao J, Chen M, Li G. Dermatopontin is a novel regulator of the CdCl2-induced decrease in claudin-11 expression. Toxicol In Vitro. 2014;28(6):1158–64. https://doi.org/10.1016/j.tiv.2014.05.013 PMID: 24909373
72. Brzoska MM, Kaminski M, Dziki M, Moniuszko-Jakoniuk J. Changes in the structure and function of the kidney of rats chronically exposed to cadmium. II. Histoenzymatic studies. Arch Toxicol. 2004;78:226–231. https://doi.org/10.1093/toxsci/kfr031
73. Babaknejad N, Moshtaghie AA, Nayeri H, Hani M, Bahrami S. Protective Role of Zinc and Magnesium against Cadmium Nephrotoxicity in Male Wistar Rats. Biol Trace Elem Res. 2016;174(1):112–20. https://doi.org/10.1007/s12011-016-0671-x PMID: 27038621
74. Koklesova L, Liskova A, Samec M, Zhai K, Al-Ishaq RK, Bugos O, et al. Protective Effects of Flavonoids Against Mitochondriopathies and Associated Pathologies: Focus on the Predictive Approach and Personalized Prevention. Int J Mol Sci. 2021;22(16):8649. https://doi.org/10.3390/ijms22168649 PMID: 34445360
75. Vargas F, Romecín P, García-Guillén AI, Wangesteen R, Vargas-Tendero P, Paredes MD, et al. Flavonoids in Kidney Health and Disease. Front Physiol. 2018;9:394. https://doi.org/10.3389/fphys.2018.00394 PMID: 29740333
76. Krstic D, Tomic N, Radosavljevic B, Avramovic N, Dragutinovic V, Skodric SR, et al. Biochemical Markers of Renal Function. Curr Med Chem. 2016;23(19):2018–40. https://doi.org/10.2174/0929867323666160115130241 PMID: 26769095
77. Gowda S, Desai PB, Kulkarni SS, Hull VV, Math AAK, Vernekar SN. Markers of renal function tests. N Am J Med Sci. 2010;2(4):170–3. PMID: 22624135
78. Cheng K, Song Z, Chen Y, Li S, Zhang Y, Zhang H, et al. Resveratrol Protects Against Renal Damage via Attenuation of Inflammation and Oxidative Stress in High-Fat-Diet-Induced Obese Mice. Inflammation. 2019;42(3):937–45. https://doi.org/10.1007/s10753-018-0948-7 PMID: 30554371
79. Aqeel T, Gurumallu SC, Bhaskar A, Hashimi SM, Javaraiah R. Secoisolariciresinol diglucoside protects against cadmium-induced oxidative stress-mediated renal toxicity in rats. J Trace Elem Med Biol. 2020;61:126552. https://doi.org/10.1016/j.jtemb.2020.126552 PMID: 32446210
80. Fernando TD, Jayawardena BM, Mathota Arachchige YLN. Variation of different metabolites and heavy metals in *Oryza sativa* L., related to chronic kidney disease of unknown etiology in Sri Lanka. Chemosphere. 2020;247:125836. https://doi.org/10.1016/j.chemosphere.2020.125836 PMID: 31931313
81. Nemmiche S. Oxidative Signaling Response to Cadmium Exposure. Toxicol Sci. 2017;156(1):4–10. https://doi.org/10.1093/toxsci/kfw222 PMID: 27803385
82. Almeer RS, AlBasher GI, Alarifi S, Alkahtani S, Ali D, Abdel Moneim AE. Royal jelly attenuates cadmium-induced nephrotoxicity in male mice. Sci Rep. 2019;9(1):5825. https://doi.org/10.1038/s41598-019-42368-7 PMID: 30967588
83. Mumtaz F, Albeltagy RS, Diab MSM, Abdel Moneim AE, El-Habit OH. Exposure to arsenite and cadmium induces organotoxicity and miRNAs deregulation in male rats. Environ Sci Pollut Res Int. 2020;27(14):17184–93. https://doi.org/10.1007/s11356-020-08306-1 PMID: 32152865
84. Sánchez M, Romero M, Gómez-Guzmán M, Tamargo J, Pérez-Vizcaino F, Duarte J. Cardiovascular Effects of Flavonoids. Curr Med Chem. 2019;26(39):6991–7034. https://doi.org/10.2174/0929867326666181220094721 PMID: 30569843
85. Kumar S, Pandey AK. Chemistry and biological activities of flavonoids: an overview. ScientificWorldJournal. 2013;2013:162750. https://doi.org/10.1155/2013/162750 PMID: 24470791
86. Arts ICW, Sesink ALA, Faassen-Peters M, Hollman PCH. The type of sugar moiety is a major determinant of the small intestinal uptake and subsequent biliary excretion of dietary quercetin glycosides. Br J Nutr. 2004;91(6):841–7. https://doi.org/10.1079/BJN20041123 PMID: 15182387
87. Cirmi S, Maugeri A, Micali A, Marini HR, Puzzolo D, Santoro G, et al. Cadmium-Induced Kidney Injury in Mice Is Counteracted by a Flavonoid-Rich Extract of Bergamot Juice, Alone or in Association with Curcumin and Resveratrol, via the Enhancement of Different Defense Mechanisms. Biomedicines. 2021;9(12):1797. https://doi.org/10.3390/biomedicines9121797 PMID: 34944613
88. Ashkar F, Bhullar KS, Wu J. The Effect of Polyphenols on Kidney Disease: Targeting Mitochondria. Nutrients. 2022;14(15):3115. https://doi.org/10.3390/nu14153115 PMID: 35956292
89. Kandemir FM, Yildirim S, Kucukler S, Caglayan C, Mahamadu A, Dortbudak MB. Therapeutic efficacy of zingerone against vancomycin-induced oxidative stress, inflammation, apoptosis and aquaporin 1 permeability in rat kidney. Biomed Pharmacother. 2018;105:981–91. https://doi.org/10.1016/j.biopha.2018.06.048 PMID: 30021393
90. Das S, Dewanjee S, Dua TK, Joardar S, Chakraborty P, Bhowmick S, et al. Carnosic Acid Attenuates Cadmium Induced Nephrotoxicity by Inhibiting Oxidative Stress, Promoting Nrf2/HO-1 Signalling and Impairing TGF-β1/Smad/Collagen IV Signalling. Molecules. 2019;24(22):4176. https://doi.org/10.3390/molecules24224176 PMID: 31752142
91. Aktoz T. Protective Effect of Quercetin Against Renal Toxicity Induced by Cadmium in Rats. Balkan Med J. 2012;29(1):56–61. https://doi.org/10.5152/balkanmedj.2011.014

92. Kim KS, Lim H-J, Lim JS, Son JY, Lee J, Lee BM, et al. Curcumin ameliorates cadmium-induced nephrotoxicity in Sprague-Dawley rats. Food Chem Toxicol. 2018;114:34–40. https://doi.org/10.1016/j.fct.2018.02.007 PMID: 29421648

93. Eldutar E, Kandemir FM, Kucukler S, Caglayan C. Restorative effects of Chrysin pretreatment on oxidant-antioxidant status, inflammatory cytokine production, and apoptotic and autophagic markers in acute paracetamol-induced hepatotoxicity in rats: An experimental and biochemical study. J Biochem Mol Toxicol. 2017;31(11):10.1002/jbt.21960. https://doi.org/10.1002/jbt.21960 PMID: 28682524

94. Yuan G, Dai S, Yin Z, Lu H, Jia R, Xu J. Sub-chronic lead and cadmium co-induce apoptosis protein expression in liver and kidney of rats. Int J Clin Exp Pathol. 2014;7(6):2905–14. PMID: 25031709

95. Bertram R, Gram Pedersen M, Luciani DS, Sherman A. A simplified model for mitochondrial ATP production. J Theor Biol. 2006;243(4):575–86. https://doi.org/10.1016/j.jtbi.2006.07.019 PMID: 16945388

96. Bruno SR, Anathy V. Lung epithelial endoplasmic reticulum and mitochondrial 3D ultrastructure: a new frontier in lung diseases. Histochem Cell Biol. 2021;155(2):291–300. https://doi.org/10.1007/s00418-020-01950-1 PMID: 33598824

97. Duann P, Lin P-H. Mitochondria Damage and Kidney Disease. Adv Exp Med Biol. 2017;982:529–51. https://doi.org/10.1007/978-3-319-55330-6_27 PMID: 28551805

98. Ijaz MU, Shahzadi S, Hamza A, Azmat R, Anwar H, Afsar T, et al. Alleviative effects of pinostrobin against cadmium-induced renal toxicity in rats by reducing oxidative stress, apoptosis, inflammation, and mitochondrial dysfunction. Front Nutr. 2023;10:1175008. https://doi.org/10.3389/fnut.2023.1175008 PMID: 37342552

99. Chen Y, Klionsky DJ. The regulation of autophagy - unanswered questions. J Cell Sci. 2011;124(Pt 2):161–70. https://doi.org/10.1242/jcs.064576 PMID: 21187343

100. Parzych KR, Klionsky DJ. An overview of autophagy: morphology, mechanism, and regulation. Antioxid Redox Signal. 2014;20(3):460–73. https://doi.org/10.1089/ars.2013.5371 PMID: 23725295

101. Thévenod F, Lee W-K. Live and Let Die: Roles of Autophagy in Cadmium Nephrotoxicity. Toxics. 2015;3(2):130–51. https://doi.org/10.3390/toxics3020130 PMID: 29056654

102. Yang F, Zhang C, Zhuang Y, Gu X, Xiao Q, Guo X, et al. Oxidative Stress and Cell Apoptosis in Caprine Liver Induced by Molybdenum and Cadmium in Combination. Biol Trace Elem Res. 2016;173(1):79–86. https://doi.org/10.1007/s12011-016-0633-3 PMID: 26883837

103. Liu F, Wang X-Y, Zhou X-P, Liu Z-P, Song X-B, Wang Z-Y, et al. Cadmium disrupts autophagic flux by inhibiting cytosolic Ca^{2+}-dependent autophagosome-lysosome fusion in primary rat proximal tubular cells. Toxicology. 2017;383:13–23. https://doi.org/10.1016/j.tox.2017.03.016 PMID: 28347754

104. Song X-B, Liu G, Liu F, Yan Z-G, Wang Z-Y, Liu Z-P, et al. Autophagy blockade and lysosomal membrane permeabilization contribute to lead-induced nephrotoxicity in primary rat proximal tubular cells. Cell Death Dis. 2017;8(6):e2863. https://doi.org/10.1038/cddis.2017.262 PMID: 28594408

105. Tu Y, Gu L, Chen D, Wu W, Liu H, Hu H, et al. Rhein Inhibits Autophagy in Rat Renal Tubular Cells by Regulation of AMPK/mTOR Signaling. Sci Rep. 2017;7:43790. https://doi.org/10.1038/srep43790 PMID: 28252052

106. Chatterjee S, Sarkar S, Bhattacharya S. Toxic metals and autophagy. Chem Res Toxicol. 2014;27(11):1887–900. https://doi.org/10.1021/tx500264s PMID: 25310621

107. Fan X, Wang J, Hou J, Lin C, Bensoussan A, Chang D, et al. Berberine alleviates ox-LDL induced inflammatory factors by up-regulation of autophagy via AMPK/mTOR signaling pathway. J Transl Med. 2015;13:92. https://doi.org/10.1186/s12967-015-0450-z PMID: 25884210

108. Kim J, Kundu M, Viollet B, Guan K-L. AMPK and mTOR regulate autophagy through direct phosphorylation of Ulk1. Nat Cell Biol. 2011;13(2):132–41. https://doi.org/10.1038/ncb2152 PMID: 21258367

109. Wargasetia TL, Shahib N, Martaadisoebrata D, Dhianawaty D, Hernowo B. Characterization of apoptosis and autophagy through Bcl-2 and Beclin-1 immunoexpression in gestational trophoblastic disease. Iran J Reprod Med. 2015;13(7):413–20. PMID: 26494988

110. Gao D, Xu Z, Kuang X, Qiao P, Liu S, Zhang L, et al. Molecular characterization and expression analysis of the autophagic gene beclin 1 from the purse red common carp (Cyprinus carpio) exposed to cadmium. Comp Biochem Physiol C Toxicol Pharmacol. 2014;160:15–22. https://doi.org/10.1016/j.cbpc.2013.11.004 PMID: 24291087

111. Zhong L, Wang L, Xu L, Liu Q, Jiang L, Zhi Y, et al. The role of nitric oxide synthase in an early phase Cd-induced acute cytotoxicity in MCF-7 cells. Biol Trace Elem Res. 2015;164(1):130–8. https://doi.org/10.1007/s12011-014-0187-1 PMID: 25510362

112. Zhu MK, Li HY, Bai LH, Wang LS, Zou XT. Histological changes, lipid metabolism, and oxidative and endoplasmic reticulum stress in the liver of laying hens exposed to cadmium concentrations. Poult Sci. 2020;99(6):3215–28. https://doi.org/10.1016/j.psj.2019.12.073 PMID: 32475458

113. Rafati Rahimzadeh M, Rafati Rahimzadeh M, Kazemi S, Moghadamnia A-A. Cadmium toxicity and treatment: An update. Caspian J Intern Med. 2017;8(3):135–45. https://doi.org/10.22088/cjim.8.3.135 PMID: 28932363

114. Souza-Arroyo V, Fabián JJ, Bucio-Ortiz L, Miranda-Labra RU, Gomez-Quiroz LE, Gutiérrez-Ruiz MC. The mechanism of the cadmium-induced toxicity and cellular response in the liver. Toxicology. 2022;480:153339. https://doi.org/10.1016/j.tox.2022.153339 PMID: 36167199